Faculty of Chemical Technology and Engineering

Research project in chemical engineering

Bachelor diploma

Aspen Plus Simulation of a Water Electrolysis System for Green Hydrogen Production: Process Design and Optimization

Hugo López García

Supervisors:
Halina Murasiewicz, PhD
Barbara Zakrzewska, PhD

Szczecin 2025

Table of Contents

Abstract

The global imperative for sustainable energy solutions positions green hydrogen, produced via water electrolysis powered by renewable electricity, as a pivotal energy carrier. This study leverages Aspen Plus simulation software to design, model, and optimize an alkaline water electrolysis (AEL) system for green hydrogen production. The research aims to evaluate system performance under various operating conditions and identify optimal parameters for efficiency and cost reduction.

The methodology involved developing a detailed Aspen Plus model, initially focusing on a simplified configuration without a circulation loop (Part I) and subsequently attempting a more complex integrated system with material recirculation (Part II). Key parameters investigated in Part I included operating temperature (70°C, 80°C, 90°C) and the number of cells per stack (12, 40, 80), all under a fixed 10 kW power input and 7 bar pressure.

Results from Part I demonstrated that the model accurately reproduces experimental data, with a Faraday efficiency of 95.21% and a voltage efficiency of 86.67% at 70°C. The optimal operating point for maximizing hydrogen production and overall efficiency was identified as 12 cells at 70°C, yielding approximately 0.104 kmol/h of hydrogen. Analysis revealed that increasing temperature, contrary to some expectations, slightly decreased total hydrogen production and overall energy efficiencies due to a notable decline in Faraday efficiency. A striking finding was the insensitivity of the total hydrogen production rate to the number of cells at a fixed total power input, indicating that cell count primarily influences the stack's voltage-current profile rather than its total output.

Part II, which incorporated a full material recirculation loop, encountered significant numerical convergence challenges. Despite employing tearing methods, the simulation yielded physically unrealistic results, including high oxygen contamination in the purified hydrogen stream, preventing successful finalization of this section.

In conclusion, while the integrated system with recirculation requires further methodological refinement, the base case simulation provides valuable insights into the optimal design and operation of AEL systems. The findings underscore the critical trade-offs between temperature, Faraday efficiency, and hydrogen output, and clarify the role of cell number in system design. This work establishes a solid foundation for future, more advanced simulations aimed at developing efficient and sustainable green hydrogen production facilities.

Keywords: Green Hydrogen, Water Electrolysis, Aspen Plus, Alkaline Electrolysis (AEL), Process Optimization

List of figures

List of tables

Symbols

Symbol	Description	Unit
E_{th}	Thermoneutral voltage	V
F_c	Faraday constant	C/mol
H_o	Higher heating value of hydrogen	J/m^3
H_u	Lower heating value of hydrogen	J/m^3
I_{cell}	Electrolyzer cell current	A
η_F	Faraday efficiency	–
η_{HHV}	Higher Heating Value efficiency	–
η_{LHV}	Lower Heating Value efficiency	–
η_V	Voltage efficiency	–
P	Pressure	bar
P_{el}	Electrical power input to the electrolyzer	W or kW
T	Temperature	°C
$\dot{m}$	Mass flow rate	kg/h
$\dot{N}$	Molar flow rate of species produced or consumed	mol/s
V_{H2}	Volumetric hydrogen flow rate	m^3/s
V_{cell}	Actual cell voltage	V

1. Introduction

The pursuit of a sustainable energy future is no longer a distant aspiration, but a pressing global imperative. As the world seeks to transition away from fossil fuels and mitigate the impacts of climate change, green hydrogen has emerged as a critical component of this transformation. Hydrogen production through electrolysis, when powered by renewable energy, offers a zero-emission alternative to conventional hydrogen production methods that rely on fossil fuels (Holladay et al., 2009). Despite its potential, green hydrogen currently accounts for less than 0.1% of total dedicated hydrogen production, but declining costs of renewable electricity are expected to accelerate its adoption (IEA, 2024).

This chapter will delve into the fundamental role of water electrolysis in green hydrogen production, examining how this technology utilizes renewable energy to split water into hydrogen and oxygen, offering a clean and sustainable alternative to traditional hydrogen production methods. Furthermore, it will provide an overview of the different water electrolysis technologies, including alkaline, proton exchange membrane (PEM), and solid oxide electrolyzers, highlighting their unique characteristics, advantages, and applications in the evolving landscape of green hydrogen production (Shiva Kumar & Lim, 2022)

Through this exploration, the aim is to illuminate the significance of green hydrogen, and the pivotal role water electrolysis plays in realizing a future powered by clean, abundant, and environmentally responsible energy. The continued development and deployment of electrolyzers, alongside advancements in materials science and policy support, will be crucial for scaling up production and making green hydrogen a competitive energy carrier (IEA, 2024).

1.1. Importance of green hydrogen in achieving a sustainable energy future

Green hydrogen stands as a pivotal pillar in the ambitious transition towards a carbon-neutral economy, a goal that increasingly dominates global energy policy and technological innovation. The role of green hydrogen in decarbonizing hard-to-abate sectors is pivotal, as it provides a clean alternative to conventional energy systems (Zhang et al., 2022). Its significance stems from its unique production method, which starkly contrasts with conventional hydrogen generation. Unlike the "gray" hydrogen, derived from fossil fuels through processes like steam methane reforming and burdened with substantial carbon dioxide emissions, or even "blue" hydrogen, which attempts to mitigate these emissions with carbon capture and storage, green hydrogen is produced through the electrolysis of water (Shiva Kumar & Lim, 2020). This

process, when powered exclusively by renewable energy sources such as solar, wind, or hydropower, ensures that the hydrogen produced carries an exceptionally low carbon footprint. Water electrolysis powered by renewable energy sources is the most sustainable method for producing hydrogen, as it generates little to no emissions during production (Dincer & Acar, 2015).

Moreover, green hydrogen plays a crucial role in the transition to net-zero emissions, as it provides a scalable solution to replace fossil fuels in sectors like transportation, industry, and power generation (IEA, 2024). This highlights the growing importance of green hydrogen in achieving long-term sustainability and reducing global carbon emissions. The ability of green hydrogen to be produced from renewable energy sources makes it an essential tool in addressing climate change and advancing the global energy transition (Shiva Kumar & Lim, 2020).

Furthermore, green hydrogen plays a crucial role in addressing the inherent intermittency of renewable energy sources. Solar and wind power, while abundant and clean, are subject to fluctuations based on weather patterns and time of day. The variability of renewable energy sources, such as wind and solar, presents challenges for maintaining grid stability (IEA, 2024). Green hydrogen, with its capacity for large-scale and long-duration storage, acts as an effective energy storage medium. Green hydrogen, produced via water electrolysis, can store surplus renewable energy during peak production and release it during periods of low renewable output (Shiva Kumar & Lim, 2020). During periods of excess renewable energy production, the surplus can be channeled into electrolyzers to generate green hydrogen, which can then be stored for later use. Green hydrogen is considered a flexible and efficient energy storage option that supports the integration of intermittent renewable energy into the power system (Zhang et al., 2022). Conversely, during periods of low renewable energy output, the stored hydrogen can be utilized to generate electricity, ensuring grid stability and reliability. Hydrogen serves as a flexible backup source for electricity generation in power systems dependent on renewables (Dincer & Acar, 2015).

However, the widespread adoption of green hydrogen is not without its challenges. Significant investments in infrastructure, encompassing electrolyzers, pipelines, storage facilities, and refueling stations, are essential to support its integration into existing energy systems. Scaling up green hydrogen production and distribution requires substantial investment in infrastructure, including the development of dedicated hydrogen transport and storage networks (IEA, 2024). Moreover, the cost of green hydrogen production needs to be reduced to make it economically competitive with fossil fuels, which can be achieved through technological advancements, economies of scale, and supportive policy frameworks. The cost

reduction of green hydrogen is fundamental for its widespread adoption, and ongoing research aims to lower production costs by improving electrolyzer efficiency and scaling up production capacities (Zhang et al., 2022).

Governments play a vital role in creating a conducive policy environment, including incentives, regulations, and standards, to drive the development and deployment of green hydrogen technologies. Governments must create a supportive policy framework, including financial incentives and regulatory measures, to facilitate the growth of the green hydrogen sector (IEA, 2024). Ongoing research and development are also crucial for improving the efficiency and durability of electrolyzer technologies and exploring innovative applications for green hydrogen across various sectors. Continuous technological innovation is key to enhancing the economic feasibility and performance of water electrolysis systems (Shiva Kumar & Lim, 2020).

In essence, green hydrogen, produced through water electrolysis powered by renewable energy, represents a transformative solution for decarbonizing hard-to-abate industries and providing essential energy storage capabilities. Green hydrogen plays a crucial role in decarbonizing sectors that are difficult to electrify, such as heavy industry and transportation, offering a clean alternative to conventional fuels (Zhang et al., 2022). Its potential to seamlessly integrate with renewable energy sources and mitigate climate change makes it a critical component of the global transition to a sustainable and carbon-neutral economy. Water electrolysis powered by renewable energy offers a sustainable pathway for hydrogen production, ensuring minimal carbon emissions and contributing to the decarbonization of the energy sector (Shiva Kumar & Lim, 2020).

1.2 Role of water electrolysis in green hydrogen production

Water electrolysis is recognized as one of the most promising and sustainable technologies for hydrogen production, marking a significant shift away from traditional, fossil fuel-dependent methods. This process involves the splitting of water molecules (H_2O) into hydrogen (H_2) and oxygen (O_2) using electricity. The crucial factor that defines green hydrogen is that the electricity used for electrolysis comes from renewable sources such as wind, solar, or hydropower. This makes the hydrogen produced entirely decarbonized, as opposed to conventional methods like steam methane reforming (SMR), which generates significant carbon emissions due to the use of fossil fuels like natural gas (Zhang et al., 2022; Franco &

Giovannini, 2023). The European production of hydrogen, based on different technologies, is depicted in Figure 1.

One of the key advantages of water electrolysis is its ability to utilize surplus renewable energy during periods of high production. Renewable energy sources like wind and solar are intermittent, and excess energy during peak production periods can be stored as green hydrogen. This hydrogen can later be used during times of low renewable energy generation, thereby stabilizing the electricity grid and addressing the challenges posed by the variability of renewable sources (Zhang et al., 2022). This characteristic of water electrolysis enhances the integration of renewable energy into the grid and ensures a more reliable and resilient energy infrastructure.

Furthermore, the production of green hydrogen via electrolysis is a transformative solution for sectors that are difficult to electrify directly, such as heavy industry and long-haul transportation. Industries like steel and cement production require high-temperature processes that are typically powered by fossil fuels. Green hydrogen can serve as a clean fuel source for these industries, enabling them to decarbonize and contribute to global climate goals (Franco & Giovannini, 2023). Additionally, hydrogen produced via electrolysis can be used in fuel cell electric vehicles (FCEVs), offering a sustainable alternative to traditional internal combustion engine vehicles and further advancing the decarbonization of the transportation sector (Zhang et al., 2022).

Water electrolysis is not only a promising hydrogen production technology but also offers scalability and flexibility. Electrolyzers can be scaled up for large-scale industrial hydrogen production or deployed in decentralized locations to serve specific needs, such as fueling stations or remote industrial applications. This flexibility enables a wide range of potential applications, making it a versatile solution for the hydrogen economy (Zhang et al., 2022). As research and development continue, advancements in electrolyzer technologies will likely improve efficiency, reduce costs, and expand the potential for green hydrogen production worldwide (Franco & Giovannini, 2023).

In conclusion, water electrolysis plays a pivotal role in the global transition to a sustainable energy system. By providing a clean, scalable, and flexible method for hydrogen production, it supports the integration of renewable energy sources, facilitates decarbonization in hard-to-abate sectors, and offers a reliable energy storage solution for the future. This makes water electrolysis an essential technology in building a low-carbon and resilient global energy infrastructure (Franco & Giovannini, 2023; Zhang et al., 2022). This relevance is further

underscored by recent data on hydrogen production capacity in Europe, as illustrated in Figure 1 from the European Hydrogen Observatory (2023).

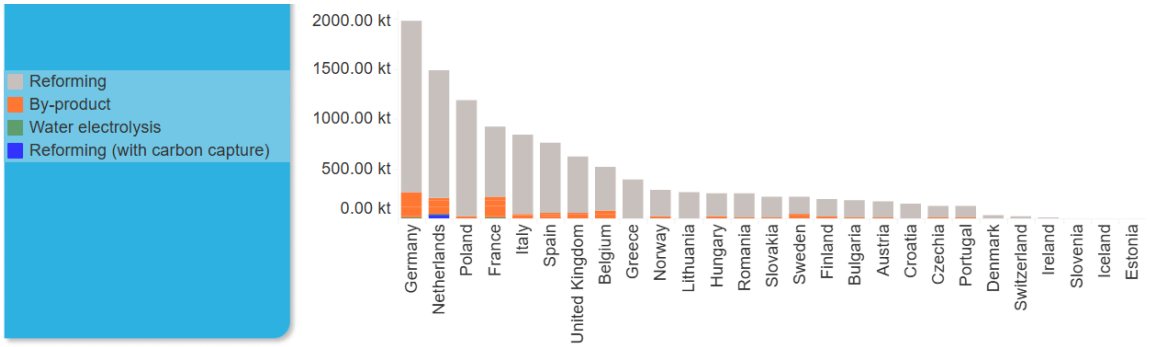

Figure 1. Total hydrogen production in Europe in 2023

1.3 Different water electrolysis technologies (alkaline, PEM, solid oxide)

Water electrolysis is a key process for green hydrogen production, enabling the decomposition of water into hydrogen and oxygen using electricity. However, not all electrolyzers function in the same way. Various technologies have been developed, each with distinct characteristics, advantages, and challenges. The most widely studied and applied technologies include Alkaline Electrolysis (AEL), Proton Exchange Membrane Electrolysis (PEM), Solid Oxide Electrolysis Cells (SOEC), and Anion Exchange Membrane Electrolysis (AEM) (Franco & Giovannini, 2023).

- **Alkaline electrolysis** is the most mature and commercially established technology. It employs a liquid electrolyte, typically potassium hydroxide (KOH) or sodium hydroxide (NaOH), and operates at temperatures between 60 and 80°C. A key advantage of AEL is its low cost since it does not require expensive noble metal catalysts. However, its efficiency is lower than other methods, and it has a slow dynamic response, making it less suitable for direct integration with intermittent renewable energy sources (Franco & Giovannini, 2023; Shiva Kumar & Himabindu, 2019).
- **Proton Exchange Membrane (PEM) Electrolysis** utilizes a solid polymer membrane as the electrolyte, enabling high efficiency (70–80%) and fast response times. Operating at moderate temperatures (50–80°C), PEM technology produces high-purity hydrogen. Its main drawback is the reliance on expensive noble metals, such as platinum and iridium, which increase production costs. Despite this, PEM electrolysis is favored in

applications requiring rapid start-up times and high operational flexibility (Franco & Giovannini, 2023; Shiva Kumar & Himabindu, 2019).

- **Solid Oxide Electrolysis Cells (SOECs)** technology operates at high temperatures (700–1000°C) using a ceramic electrolyte. It offers the highest efficiency (>90%) due to its ability to utilize excess thermal energy from industrial processes. However, the extreme operating conditions pose challenges related to material degradation and thermal management, limiting its widespread commercialization (Franco & Giovannini, 2023; Jang et al., 2021). SOECs are particularly promising for industrial applications where waste heat is available to enhance efficiency.
- **Anion Exchange Membrane (AEM) Electrolysis** is an emerging technology that combines the advantages of AEL and PEM. It uses a solid polymer membrane that transports hydroxide ions (OH^-) instead of protons (H^+), eliminating the need for highly concentrated liquid electrolytes (as in AEL) while avoiding the expensive noble metal catalysts used in PEM. Although still in the research and development stage, AEM technology has demonstrated potential for cost reduction and improved efficiency (González-Elipe & de Lucas-Consuegra, 2021).

Comparison and Future Perspectives

AEL and PEM electrolysis are the most commercially developed and widely used technologies. However, SOEC and AEM are gaining interest due to their higher efficiencies and potential cost reductions. Current research efforts focus on improving electrolyzer materials, enhancing operational durability, and increasing integration with renewable energy sources. The development of scalable, cost-effective, and high-efficiency electrolysis technologies is crucial for the large-scale deployment of green hydrogen production and achieving global decarbonization goals (Franco & Giovannini, 2023; Shiva Kumar & Himabindu, 2019).

1.4. Advantages of using renewable energy sources for electrolysis

The integration of renewable energy sources with water electrolysis presents a pathway toward truly sustainable hydrogen production. This approach not only enables the decarbonization of hydrogen generation but also contributes to the broader transition toward a resilient, low-carbon energy system. The benefits of using renewables in electrolysis are both

environmental and strategic and are increasingly recognized in scientific research and global energy strategies.

Zero Greenhouse Gas Emissions

When powered by renewable energy sources such as wind, solar, or hydropower, water electrolysis becomes a completely emissions-free process. This is in stark contrast to traditional hydrogen production methods like steam methane reforming (SMR), which emit significant amounts of CO_2 (IEA, 2024). By utilizing renewable electricity, green hydrogen production avoids lifecycle greenhouse gas emissions and supports climate targets, including those set in the Paris Agreement (IEA, 2022; Shiva Kumar & Himabindu, 2019).

Grid Balancing and Load Flexibility

Electrolyzers can operate dynamically, adjusting their consumption based on electricity availability. This flexibility allows them to absorb excess electricity during periods of high renewable generation and reduce load during shortages, thus stabilizing grids with large shares of intermittent resources like wind and solar (IEA, 2022; Zhang et al., 2022). Research has shown that demand-side management with flexible electrolyzers contributes significantly to maintaining grid stability and improving renewable energy integration (Jang et al., 2021).

Energy Storage and Sector Coupling

Hydrogen acts as a long-duration energy storage medium, enabling the conversion of surplus renewable electricity into chemical energy. This stored hydrogen can be used later in fuel cells, combustion turbines, or industrial applications, effectively decoupling electricity generation from consumption timeframes (Franco & Giovannini, 2023). In this way, green hydrogen contributes to sector coupling—connecting the electricity sector with transportation, industry, and heating—thus improving the overall efficiency and sustainability of the energy system (IRENA, 2022).

Energy Independence and Security

Producing hydrogen locally with domestic renewable energy reduces dependence on fossil fuel imports, enhancing energy security. This is especially critical for countries with limited natural gas or oil reserves. Decentralized hydrogen production based on renewables also supports rural development and job creation in regions rich in solar or wind resources (González-Elipe & de Lucas-Consuegra, 2021).

Additional Environmental and Economic Benefits

The integration of renewables with electrolysis helps reduce air pollution and water consumption compared to fossil-based hydrogen. Moreover, as the costs of solar PV and wind energy continue to decline, and electrolyzer technologies advance, green hydrogen is expected to become increasingly cost-competitive with gray and blue hydrogen (IEA, 2022; Franco & Giovannini, 2023).

1.5. The need for process simulation and optimization to improve efficiency and reduce costs

The global urgency to shift away from fossil fuels and towards sustainable energy alternatives has positioned hydrogen as a cornerstone of future energy systems. Within this emerging hydrogen economy, green hydrogen—produced via water electrolysis powered by renewable energy sources—offers a transformative solution to mitigate climate change and reduce environmental degradation. Among the various electrolysis technologies available, Alkaline Electrolysis (AEL) stands out due to its technological maturity, economic feasibility, and scalability, making it especially well-suited for large-scale hydrogen production (Zhang et al., 2022; IRENA, 2020).

The integration of renewable energy sources such as solar, wind, hydropower, and geothermal with AEL enables hydrogen production with minimal to zero greenhouse gas emissions. This green pathway contrasts sharply with conventional methods like steam methane reforming (SMR), which are associated with high carbon dioxide emissions and dependency on finite fossil fuel resources (IEA, 2022; Shiva Kumar & Himabindu, 2019). By eliminating emissions during the hydrogen generation process, green hydrogen production through AEL contributes directly to achieving global carbon neutrality goals (Franco & Giovannini, 2023).

In addition to its environmental benefits, renewable energy-driven electrolysis supports long-term sustainability. Unlike fossil fuels, renewables are naturally replenishing and widely distributed, minimizing ecological disturbances and avoiding air and water pollution associated with fossil fuel extraction and combustion. This results in reduced environmental degradation, healthier ecosystems, and a lower ecological footprint overall (IRENA, 2022; González-Elipe & de Lucas-Consuegra, 2021).

Another major advantage of coupling renewable energy with AEL is the enhancement of energy security. Hydrogen produced in this way reduces dependence on volatile fossil fuel markets and mitigates geopolitical risks linked to energy imports. Moreover, the decentralized nature of renewable energy systems allows electrolyzers to be deployed locally, empowering regional and even off-grid hydrogen production. This flexibility not only lowers the need for long-distance energy transport but also reinforces local energy autonomy, contributing to a more resilient and diversified energy supply (IEA, 2024; Zhang et al., 2022).

Furthermore, AEL systems are particularly attractive for renewable integration due to their compatibility with intermittent power sources. Although AELs generally respond more slowly to load fluctuations than PEM electrolyzers, ongoing advancements are improving their dynamic response, thereby enhancing their suitability for pairing with solar and wind energy (Franco & Giovannini, 2023). Their long operational lifespans, use of inexpensive and abundant materials (such as nickel and stainless steel), and low capital costs further contribute to their appeal in both developed and developing markets (IRENA, 2022).

Finally, to fully leverage the potential of AEL and renewable energy integration, simulation and process optimization play a vital role. Advanced modeling techniques using tools like Aspen Plus or MATLAB allow engineers to fine-tune operational parameters such as voltage, temperature, and flow rates, thereby maximizing hydrogen yield and minimizing energy consumption. Optimization not only reduces operational costs but also improves system durability and performance under fluctuating renewable energy inputs (Jang et al., 2021).

In conclusion, the convergence of renewable energy technologies and AEL presents a promising pathway for producing sustainable, low-cost hydrogen. As innovations continue to drive down costs and improve system efficiencies, green hydrogen will play a pivotal role in shaping a decarbonized, secure, and resilient global energy system.

Economic, Operational, and Technical Benefits of Renewable Energy-Powered Electrolysis

In addition to its well-documented environmental and energy security advantages, renewable energy-powered electrolysis provides substantial grid flexibility and stabilization benefits. One of the key advantages lies in its ability to utilize excess renewable electricity that would otherwise be curtailed during periods of low demand and high generation. By operating as a

flexible demand-side technology, electrolysis can absorb surplus energy from variable sources like wind and solar, thereby helping to stabilize the grid and improve its reliability (IEA, 2022; Zhang et al., 2022).

Moreover, hydrogen produced via electrolysis offers a long-term energy storage solution. Unlike batteries, which are suited for short-term balancing, hydrogen can be stored for weeks or months and later used in power generation, transport, or industry. This characteristic is particularly valuable in decarbonized energy systems with a high share of intermittent renewables, where seasonal storage and grid backup are essential (IRENA, 2022; Jang et al., 2021). By converting renewable electricity into hydrogen, the system gains a buffer that helps mitigate fluctuations in renewable output, enhancing energy resilience and supply continuity.

From an economic perspective, the development of a green hydrogen economy also brings considerable opportunities. The hydrogen sector is expected to create millions of jobs across the value chain—including in renewable energy production, electrolyzer manufacturing, infrastructure deployment, and hydrogen logistics (IEA, 2023). Additionally, localized hydrogen production can stimulate regional development and promote technological innovation, further contributing to economic growth and energy independence (IRENA, 2020).

As renewable energy technologies and electrolyzers evolve, the cost of green hydrogen is projected to decrease significantly. Economies of scale, technological learning, and supportive policies are key enablers of this downward trend. For instance, the cost of alkaline electrolyzers has already dropped by over 60% in the past decade and is expected to decline further, especially with increased automation and mass production (Franco & Giovannini, 2023; IRENA, 2022).

To unlock the full potential of systems like Alkaline Electrolysis (AEL), the role of process simulation and optimization becomes indispensable. Simulation tools such as Aspen Plus, MATLAB/Simulink, or COMSOL Multiphysics allow engineers to create detailed models of electrolyzer systems, enabling a better understanding of electrochemical behavior, heat and mass transfer, and fluid dynamics. These insights are crucial for optimizing operating conditions—including temperature, pressure, current density, electrolyte concentration, and flow rates—to maximize hydrogen yield and minimize energy losses (Jang et al., 2021; Shiva Kumar & Himabindu, 2019).

Additionally, process optimization leads to tangible reductions in operational costs. Accurate simulation allows for right-sizing equipment, preventing oversizing and reducing capital investment. It also assists in material savings, by minimizing the use of expensive catalysts (e.g., platinum or iridium) and reducing wear on components, thus extending system lifespan and lowering maintenance costs (Zhang et al., 2022; Franco & Giovannini, 2023).

Beyond efficiency and cost, simulation enhances system safety and reliability. By modeling transient behaviors and failure scenarios (e.g., gas leaks, overheating), it can be designed and implemented robust safety protocols. Moreover, process stability can be improved through the development of advanced control strategies, which enable automated and adaptive system operation, reducing the reliance on human intervention and minimizing downtime (Jang et al., 2021).

In essence, the integration of renewable energy with advanced electrolysis systems—supported by rigorous process simulation—forms the backbone of an efficient, sustainable, and economically viable hydrogen economy.

The Role of Process Simulation in Scaling and Optimizing AEL Systems

One of the most significant advantages of process simulation in the context of alkaline water electrolysis (AEL) is its ability to predict system behavior at large scale based on laboratory or pilot-scale data. This predictive capability is crucial for scaling up electrolysis systems efficiently and accurately, reducing the risk and cost of commercial deployment (Zhang et al., 2022; Jang et al., 2021). Simulation tools allow engineers to extrapolate performance under varying conditions, ensuring that the transition from Research and Development (R&D) to industrial applications is both technically and economically feasible.

Moreover, simulation platforms facilitate the testing and validation of novel design configurations and operating strategies before any physical implementation takes place. This virtual prototyping reduces development timelines, minimizes capital expenditure, and prevents costly trial-and-error procedures in physical setups (Shiva Kumar & Himabindu, 2019).

In systems powered by intermittent renewable energy sources, such as solar or wind, process simulation becomes even more critical. The fluctuating nature of these inputs requires AEL systems to operate dynamically and adaptively. Dynamic simulation models enable to analyze the response of electrolyzers to real-time changes in power supply, ensuring stable, efficient

hydrogen production while avoiding issues such as voltage spikes, gas crossover, or material degradation (IRENA, 2020; Franco & Giovannini, 2023). These models also help assess the interaction between AEL units and the power grid, optimizing grid integration and supporting demand-side management strategies (IEA, 2022).

Despite the many benefits of green hydrogen, its production via electrolysis still faces challenges, primarily:

- High capital costs of electrolyzers and renewable energy infrastructure.
- High energy consumption, especially under suboptimal conditions.
- Operational inefficiencies due to variable loads and design limitations.

Simulation and optimization techniques help overcome these barriers by providing:

- Enhanced system design: Identifying optimal conditions for temperature, pressure, current density, and electrolyte concentration improves overall system performance (Zhang et al., 2022).
- Reduced energy input: Simulation allows for the minimization of electricity consumption while maximizing hydrogen output through efficient operating strategies (Franco & Giovannini, 2023).
- Lower overall costs: Economic modules within simulation software can perform cost-benefit analyses, enabling stakeholders to evaluate investment feasibility and identify areas for cost savings (IRENA, 2022).
- Optimized integration with renewables: By modeling variability in electricity supply, simulation ensures robust and efficient operation under dynamic conditions (Jang et al., 2021).

A key tool in this domain is Aspen Plus, a widely adopted process simulation software that is particularly well-suited to modeling green hydrogen production systems. Aspen Plus provides detailed thermodynamic modeling, equipment sizing, sensitivity analysis, and process optimization, all of which are essential for developing economically and energetically viable AEL systems (Shiva Kumar & Himabindu, 2019). Its ability to simulate both steady-state and dynamic behavior, combined with integrated economic evaluation capabilities, makes it invaluable in assessing system feasibility under a range of scenarios.

For this study, Aspen Plus is employed to model and simulate alkaline electrolysis for hydrogen production. The platform's capabilities allow for the exploration of different operating conditions and their impact on hydrogen yield, energy consumption, and cost efficiency. Aspen Plus allows to identify optimal process parameters and understand how AEL can be most effectively integrated into renewable energy-powered systems.

Why Aspen Plus for Green Hydrogen Production Modeling?

In the pursuit of a sustainable hydrogen economy, Aspen Plus has emerged as a key simulation platform for analyzing and optimizing green hydrogen production systems, particularly those based on alkaline electrolysis (AEL). As the complexity of integrating electrolysis with intermittent renewable energy sources increases, advanced simulation tools become essential to ensure technical, economic, and operational viability. Aspen Plus offers a comprehensive environment for modeling both steady-state and dynamic behaviors of electrolyzer systems, making it an indispensable tool in the design and optimization of green hydrogen infrastructure.

1. Comprehensive Thermodynamic Modeling

Aspen Plus provides highly accurate thermodynamic frameworks that are essential for describing phase equilibria, reaction kinetics, and heat/mass transfer in electrolysis processes (Franco & Giovannini, 2023). These capabilities are particularly useful when evaluating how operating conditions—such as temperature, pressure, and electrolyte concentration—affect hydrogen yield and energy efficiency. Additionally, users can implement custom electrochemical models for specific technologies including AEL, PEM, SOEC, and AEM, allowing for flexibility in research and industrial applications (Shiva Kumar & Himabindu, 2019).

2. Integration with Renewable Energy Sources

Hydrogen production via electrolysis is increasingly linked to intermittent renewable energy like solar and wind. Aspen Plus enables detailed scenario analysis, allowing researchers to model system responses to varying electricity inputs. These simulations are crucial for understanding how fluctuations in renewable generation impact electrolyzer performance and system stability (IRENA, 2020). The software also supports energy integration studies,

enabling scientist to evaluate and optimize thermal management strategies, heat recovery, and overall energy utilization (Zhang et al., 2022).

3. Dynamic Behavior Simulation

Modern electrolysis systems must operate under transient conditions, especially when coupled with variable renewables. While Aspen Plus is traditionally known for steady-state modeling, it can also be linked with dynamic simulation tools (e.g., Aspen Dynamics or MATLAB-Simulink) to analyze real-time behavior, load-following capabilities, and control strategies (Jang et al., 2021). This is critical for ensuring operational stability and process resilience under real-world conditions.

4. Economic Evaluation and Process Optimization

Aspen Plus features built-in cost estimation and economic analysis modules that support techno-economic assessments of green hydrogen projects. It enables sensitivity analysis to evaluate how key parameters—such as electricity price, operating temperature, and water cost—impact the Levelized Cost of Hydrogen (LCOH) (IEA, 2022). Through optimization, it is possible to identify cost-saving strategies, including optimal equipment sizing, catalyst usage, and utility consumption, making green hydrogen more competitive with fossil-based alternatives (Franco & Giovannini, 2023).

5. Scalability and Industrial Application

From laboratory to industrial scale, Aspen Plus offers multi-scale modeling capabilities. It allows operators to simulate small pilot systems and extrapolate to large-scale deployments, supporting feasibility studies, system design, and process scale-up. This is especially important for projects seeking to transition from research and development to commercial implementation (Zhang et al., 2022; IEA, 2023). Moreover, Aspen Plus facilitates techno-economic optimization, providing stakeholders with critical insights to support investment decisions and policy planning.

In conclusion, the utilization of renewable energy sources for electrolysis, particularly in conjunction with AEL technology, offers a compelling pathway towards a sustainable hydrogen economy. However, to fully realize its potential, process simulation and optimization are indispensable tools. By enabling a deeper understanding of process dynamics, optimizing

operating parameters, and improving equipment design, these techniques play a critical role in making green hydrogen a viable and competitive energy carrier. As it continues to innovate and refine these technologies, the move closer to a future powered by clean, abundant, and environmentally responsible energy.

2. Literature Review

Green hydrogen, produced through water electrolysis using renewable energy, is a key component of a sustainable energy future. To realize the full potential of this technology, efficient and optimized process designs are essential. This literature review investigates the green hydrogen production and the use of Aspen Plus, a comprehensive process simulation tool, for the design and optimization of water electrolysis systems. The review will analyze how Aspen Plus can be employed to improve process performance, minimize energy consumption, and scale up production.

2.1 Green Hydrogen Production

Because hydrogen is primarily found in chemical compounds on Earth, it must be extracted to be used as an energy carrier. The two main extraction methods are water splitting and extraction from organic, hydrocarbon-based compounds. Water is an especially attractive source because it is abundant and produces only hydrogen and oxygen when split. In contrast, extracting hydrogen from hydrocarbons inevitably results in CO2 emissions, unless the carbon is captured and stored effectively (Younas et al., 2022).

Currently, 95% of the world's hydrogen is derived from fossil fuels. This “grey” hydrogen production releases significant CO2, making it unsustainable for a hydrogen-based economy (International Energy Agency [IEA], 2022; (Zhang et al., 2021). “Blue” hydrogen, where these emissions are captured and stored, is a potential alternative. However, it is not entirely CO2-neutral due to emissions from fossil fuel extraction. Some regions are also exploring nuclear energy for hydrogen production, but this approach faces challenges related to public acceptance, radioactive waste disposal, and reliance on finite resources (Ahn et al., 2023; AlHumaidan et al., 2023).

“Green” hydrogen, produced solely from water, renewable biomass, and renewable energy, is essential for a sustainable hydrogen economy. Consequently, there is significant research interest in developing green hydrogen production methods, particularly electrochemical and thermochemical water splitting (Amini Horri & Ozcan, 2024).
Until renewable energy capacities are fully developed, it is also crucial to reduce emissions from current hydrogen production methods. This can be achieved by improving the efficiency of fossil fuel use and adapting these methods to utilize biomass feedstocks.

The decreasing cost of renewable energy suggests that, with continued research and supportive policies, renewable green hydrogen has the potential to become cost-competitive. Advances in hydrogen production technologies are a critical step towards a sustainable, low-carbon energy future.

2.1.1 Review the latest advancements in green hydrogen production technologies, focusing on the integration of water electrolysis with renewable energy sources.

The growing global emphasis on decarbonization has elevated green hydrogen to an important position in sustainable energy strategies. Green hydrogen is essential for reducing carbon emissions in sectors difficult to electrify, such as heavy industries and long-distance transport. In recent years, advancements have been made in electrolysis technologies and their integration with renewable energy systems.

Electrolysis is currently the most advanced and economically viable method for producing green hydrogen from water (Franco & Giovannini, 2023; El-Shafie, 2023; Nasser et al., 2022). There are significant plans to expand electrolysis capacities, enabling hydrogen generation using electricity from renewable sources (Brauns & Turek, 2020; Burton et al., 2021; Jaradat et al., 2022; Shiva Kumar & Lim, 2022) . However, thermochemical processes offer the potential for greater efficiency and more effective land use. These processes, which use high-temperature heat instead of electricity to split water, can be efficiently powered by concentrated solar thermal energy (Budama et al., 2023; Warren & Weimer, 2022; Das & Peu, 2022). This approach is particularly well-suited for sun-rich regions, and with several pilot plants already in operation, thermochemical methods are poised to play a major role in long-term hydrogen production (Boretti, 2022).

Advancements in Water Electrolysis Technologies

Water electrolysis has been identified as the most promising route for green hydrogen production. This process involves the use of electricity to split water molecules into hydrogen (H_2) and oxygen (O_2). When renewable energy powers this process, the hydrogen produced is considered completely clean, as it generates no greenhouse gas emissions. Recent research has shown that the efficiency of electrolysis systems has considerably improved through the optimization of electrodes, electrolytes, and operating conditions (Zeng & Zhang, 2022). Moreover, they are also focused on minimizing production costs and enhancing scalability to ensure that green hydrogen is competitively positioned against hydrogen derived from fossil

fuels (Rehman, 2023; Sugawara et al., 2023; Liang et al., 2023). In alkaline electrolysis (AEL), efforts have focused on enhancing electrode materials, improving membrane durability, and developing dynamic operating protocols to better handle intermittent renewable energy inputs (Franco & Giovannini, 2023). Recent advancements focus on enhancing current density and facilitating the integration of AWE technologies with renewable energy sources through sophisticated power electronics (Selvam et al., 2025).

For proton exchange membrane (PEM) electrolyzers, advancements include the reduction of precious metal catalyst loading, the introduction of more durable membranes, and improved stack designs that increase efficiency while lowering overall system costs (Zhang et al., 2022). Scientists are exploring alternatives to iridium oxide catalysts for the oxygen evolution reaction (OER), such as novel ruthenium-based compounds, and seeking to replace platinum with more affordable and stable nickel alloys on the cathode side. The Power-to-X roadmap anticipates that these materials innovations, combined with advances in manufacturing and cell design, will significantly reduce system costs, targeting a decrease from the current $1000–$1500/kW range to under $800/kW by 2030 (Genovese et al., 2023; Alhadhrami et al., 2024).

Solid oxide electrolysis cells (SOEC) have progressed through the development of novel ceramic materials and innovative cell architectures that reduce degradation rates at high temperatures, making long-term operation more viable (Franco & Giovannini, 2023). Recent academic research highlights how hybrid Solid Oxide Electrolysis (SOE) and Concentrated Solar Power (CSP) systems can further reduce electricity use by utilizing stored solar thermal energy. Despite their impressive efficiency, SOEs face key challenges, notably material costs and the intricacies of thermal management. The Power-to-X strategy aims to lower SOE expenses from the present $1500-$2000 per kilowatt to under $1200 per kilowatt by improving electrode microstructures and increasing resistance to thermal cycling (Matheswaran, 2023).

Across all technologies, emphasis is placed on cost reduction, operational flexibility, and integration capabilities with renewable energy sources, aiming to accelerate the transition from laboratory-scale demonstrations to commercial applications (IRENA, 2022).

Integration with Renewable Energy Sources

Integrating electrolysis with renewable energy presents both opportunities and challenges. Solar, wind, and hydropower are primary renewable energy sources used to power electrolysis.

This process uses electricity to split water into hydrogen and oxygen. When the electricity comes from renewable sources, the resulting hydrogen is considered "green" (GH). Electrolysis powered by wind or solar energy stands out as a top method for producing green hydrogen (GH) (Vilbergsson et al., 2023). Recent years have seen researchers making strides in the scalability, affordability, and efficiency of GH production (Boretti, 2020; Neofytidis et al., 2023). Alkaline Water Electrolysis (AWE) and Proton Exchange Membrane Water Electrolysis (PEMWE) are well-established technologies. Solid Oxide Electrolysis Cells (SOEC) are now ready for demonstration and commercialization. Anion Exchange Membrane Electrolysis (AEM) is a newer technology still in early development (Vilbergsson et al., 2023; Ahanem et al., 2023). Beyond these, emerging alternatives include direct air electrolyzers (DAE), hydroxide exchange membrane electrolyzers (HEMEs), biomass electrolysis, electrified steam methane reforming (ESMR), protonic ceramic electrochemical cell (PCEC) membrane-less electrolysis, and redox decoupling (Ioannidou et al., 2018; Bhattacharyya et al., 2017).

Integrating renewable energy is essential for green hydrogen (GH) production. It not only lowers carbon emissions but also tackles the variability of renewable sources like wind and solar power (Carlson et al., 2023). This eco-friendly approach has the potential to decarbonize transportation, industry, and electricity generation, making it a flexible solution for a cleaner, more sustainable future (Gholami & Pirsaheb, 2021). Combining renewable energy with H_2 production marks a significant move in this direction.

Generating green hydrogen (GH) using solar energy can be achieved through three main approaches: electrochemical, thermal, and photoelectrochemical methods (Kiessling et al., 2021). In the electrochemical method, photovoltaic (PV) panels are connected to an electrolyzer via a power conditioning unit that includes a maximum power point tracking (MPPT) system and a DC/DC converter. This setup optimizes output and manages the input power (Arat et al., 2020). Here, solar cells generate electricity, which then powers an external electrolyzer to split water into hydrogen (H_2) and oxygen (O_2) at the cathode and anode, respectively. The thermal method employs concentrated solar power to harness solar radiation heat. This heat drives power cycles, such as the Organic Rankine Cycle (ORC), which in turn power a high temperature electrolyzer to split water into H_2 and O_2. Finally, the photoelectrochemical (photocatalysis) method directly uses solar energy to split water. This process involves activating a photo-material, which generates photoexcited charge carriers, facilitating H_2

production through a relatively simple mechanism (Ding et al., 2020). The adaptive hydrogen buffering (AHB) framework is shown in Figure 2.

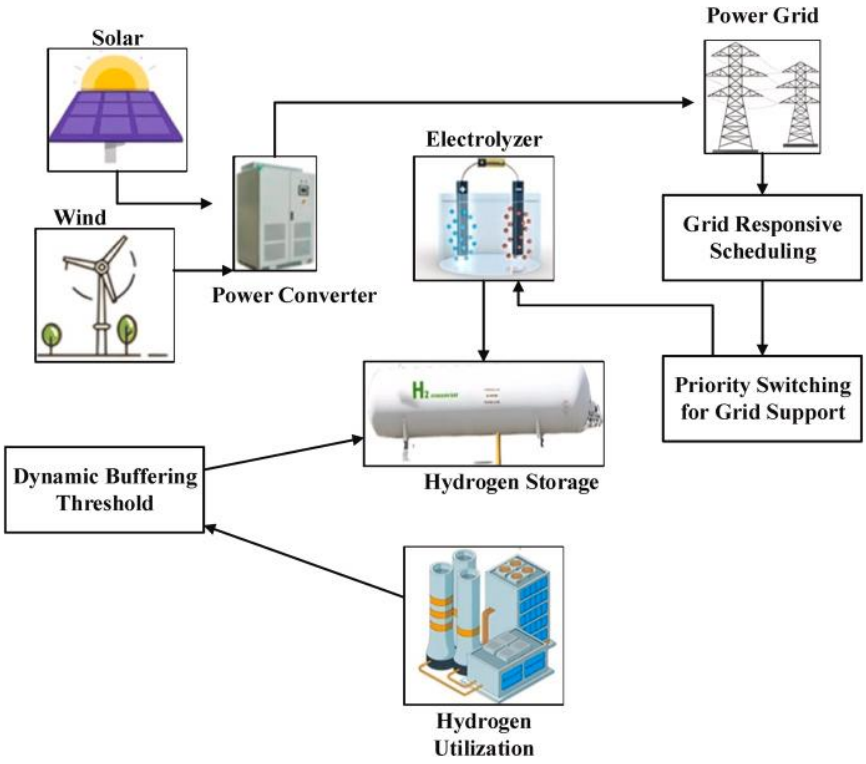

Figure 2. Adaptive Hydrogen Buffering framework; the system consists of three main elements: dynamic buffering thresholds, priority switching, and grid-responsive scheduling.

Unlike fossil fuels, renewable energy sources are variable, requiring electrolyzers to operate flexibly.

Managing Renewable Variability

While renewable energy sources like solar and wind offer a clean and sustainable path forward, their inherent variability presents considerable challenges for grid stability. Solar power generation is intrinsically tied to daylight hours and is susceptible to fluctuations caused by cloud cover and seasonal changes. Likewise, wind power output is dictated by wind speeds, which can be highly unpredictable and subject to both short-term gusts and longer-term seasonal patterns. This intermittency can result in periods of significant energy surplus during optimal conditions, followed by periods of substantial energy deficit when these conditions wane.

To guarantee the safety, reliability, and efficiency of power operations in a grid increasingly reliant on renewables, the implementation of flexible response mechanisms is paramount. The capacity to effectively store excess energy generated during peak production times and to seamlessly compensate for energy shortfalls during periods of low generation is absolutely critical for establishing a stable and dependable renewable energy grid (Habour et al., 2025). Effective integration demands that electrolysis systems adapt to fluctuating electricity supplies without compromising efficiency. Dynamic operating strategies and energy management systems are critical for maintaining stable hydrogen production (Jang et al., 2021).

Enhancing Grid Flexibility

Integrating renewable energy into networks with limited capacity necessitates robust grid flexibility. Traditionally, adaptable resources such as hydroelectric power and battery storage have played a vital role in balancing electricity supply and demand. However, while effective, these solutions often face limitations due to environmental regulations, high costs, and geographical suitability. For instance, hydroelectric reservoirs, which can absorb surplus wind energy, are constrained by ecological considerations and seasonal water availability, particularly in regions like Scandinavia where operational flexibility is restricted (Camargo et al., 2024). Similarly, although efficient for short-term balancing, battery storage frequently becomes economically unviable for long-duration energy storage due to substantial upfront and operational costs. Electrolyzers can serve as controllable loads, helping to stabilize electrical grids with high shares of renewables. By consuming surplus electricity, they prevent renewable curtailment and contribute to grid resilience (IRENA, 2022).

Energy Storage Functionality:

A major hurdle in producing green hydrogen from renewables lies in the intermittent nature of solar and wind energy. Solar photovoltaic (PV) systems only operate during daylight and are affected by cloud cover, while wind energy often fluctuates and varies with the seasons. This inconsistency reduces the effectiveness of water electrolysis, as electrolyzers require a steady and uninterrupted power supply to function optimally (Dufo-López et al., 2024). Green hydrogen provides a means of long-term energy storage, addressing the seasonal intermittency of solar and wind resources. Hydrogen can be stored and later converted back into electricity, used in industrial processes, or distributed for mobility applications (IRENA, 2022; Camargo et al., 2024).

Emerging Innovations in Green Hydrogen Production

Research has also explored novel approaches to expand the potential of green hydrogen:

1. **Seawater Electrolysis (SWE):**

Direct seawater electrolysis has gained attention to bypass the energy-intensive desalination step. Innovations focus on developing selective membranes and catalysts (active, stable, and selective) that resist chloride corrosion and minimize side reactions (Franco & Giovannini, 2023). A strategic approach, like adding a Lewis acid layer to various conventional catalysts, enables us to fine-tune their local reaction microenvironment for improved SWE. Crucially, this overarching strategy should be applicable to a wide range of catalysts, eliminating the need for specific designs tailored to individual catalysts or electrolyzer setups. Moreover, it's vital to continue stability testing until the catalyst fails. This will allow researchers to accurately determine the maximum stable operating conditions and facilitate meaningful comparisons between different catalysts (Mishra, Park, El-Mellouhi, & Han, 2024).

Innovations are currently focusing on modulating material morphology, introducing heteroatoms, and architecting heterostructures. The goal is to leverage a cooperative effect that enhances performance during electrocatalysis (Haq & Haik, 2022; Mishra, Park, El-Mellouhi, & Han, 2024; Gao, Yu, & Gao, 2022). Significant scientific and technological advancements are currently underway to reduce the cost and complexity associated with both the production and distribution of green hydrogen, particularly when generated from solar and wind energy. These efforts aim to make renewable hydrogen a more economically viable and widely accessible energy carrier.

For Solar Water Electrolysis (SWE), the long-term operational costs of an electrolyzer, which include component repairs, replacements, electricity consumption, and the expenses associated with hydrogen drying, cleaning, compression, and transportation, are projected to decrease over time (Mishra, Park, El-Mellouhi, & Han, 2024).

2. **Hybrid Renewable Systems:**

Combining multiple renewable sources, such as solar and wind, can provide a more stable and predictable electricity supply for electrolysis. Hybrid systems optimize resource utilization and improve overall hydrogen production efficiency (IRENA, 2022).

Solar energy is recognized as a renewable energy source with significant potential, largely due to its abundant solar insolation (Rahmouni et al., 2014). Researchers have estimated the potential for hydrogen (H_2) production across different regions by utilizing various renewable sources, including hydro, ocean, biomass, solar, geothermal, and wind energies (Hindson & James, 2024). For example, Rahmouni et al. (Rahmouni et al., 2014) investigated green hydrogen (GH) production in Algeria, specifically considering solar and wind energy, and their findings demonstrated that water splitting powered by renewable electricity can generate H_2.

Given global efforts to combat climate change and transition to sustainable energy, it's crucial to thoroughly understand the complexities of integrating renewable energy sources for GH production. Without adequately addressing the life cycle analysis of GH production, discussions about the significance of H_2 as a future energy source would be unproductive.

3. High-Efficiency Materials:

Advanced catalysts, new electrolyte formulations, and optimized cell architectures have pushed water electrolysis efficiency closer to theoretical limits, reducing the required energy input per kilogram of hydrogen produced (Zhang et al., 2022). For instant, perovskite (PSK) materials are highly promising for hydrogen gas generation across various processes, including photocatalytic (PC), electrocatalytic (EC), photoelectrochemical (PEC), and thermochemical catalytic (TC) (Al-Gamal et al., 2024). This is due to their unique properties that align perfectly with the demands of energy conversion involving charge separation (Shang et al., 2019).

Industrial and Policy Developments

According to the European Commission (2024), the development of renewable hydrogen is a top priority for the European Union. As outlined in the 2022 REPowerEU Strategy, the EU has set an ambitious target to domestically produce 10 million tonnes and import an additional 10 million tonnes of renewable hydrogen by 2030. Looking further ahead, renewable hydrogen is projected to satisfy approximately 10% of the EU's total energy needs by 2050. This significant integration is expected to lead to substantial decarbonization across energy-intensive industrial processes and the transport sector. Ultimately, hydrogen is recognized as a pivotal component within the EU's broader strategy for energy transition, achieving net-zero emissions, and fostering sustainable development.

The foundation of the European hydrogen policy framework was laid by the Commission in July 2021, as part of the pivotal "Fit for 55 package."

This framework incorporates binding targets for the uptake of renewable hydrogen in both industry and transport by 2030, integrated within the revised Renewable Energy Directive, which came into force in 2023. Recent guidance has been issued to assist Member States and other stakeholders in meeting these targets by May 21, 2025. Additionally, the Hydrogen and decarbonized gas market package, effective since 2024, is now in place to support the development of optimal, dedicated infrastructure for hydrogen and to foster an efficient hydrogen market.

Large-scale green hydrogen projects are rapidly emerging, supported by both private investment and government initiatives. For instant, Iberdrola's Puertollano Project is the example of the largest plant producing green hydrogen for industrial use in Europe:

Iberdrola's Puertollano Project

One of Europe's largest green hydrogen production facilities combines a 100 MW photovoltaic plant with a 20 MW electrolyzer, demonstrating the feasibility of integrated renewable-hydrogen systems at commercial scale (IEA, 2024). This facility, already one of the most efficient in the European Union with an annual production exceeding 200,000 tons, will be upgraded by Fert Iberia. The modifications will enable the plant to utilize green hydrogen for manufacturing green fertilizers. This innovative technology is projected to reduce the plant's natural gas consumption by over 10%, establishing Fertiberia as the first European company in its sector to achieve expertise in large-scale green ammonia production (Iberdrola, n.d.).

Strategic Roadmaps and Incentives

International organizations such as the IEA and IRENA have published roadmaps promoting green hydrogen adoption. Subsidies, tax credits, and research grants are increasingly directed at lowering production costs and expanding infrastructure (IEA, 2024; European Commission, 2020).

Challenges and Future Outlook

Despite considerable progress, green hydrogen production through electrolysis still faces technical and economic hurdles:

1. **Cost Reduction:**

Although electrolyzer costs are declining, achieving cost-competitive green hydrogen remains a priority. Advances in system design, materials science, and operational strategies are essential for further cost reductions (Bhuiyan & Siddique, 2025).

2. **Infrastructure Development:**

Comprehensive hydrogen supply chains, including transport, storage, and distribution infrastructure, must be developed to enable widespread hydrogen utilization. For example, efficient storage solutions are crucial across various industrial, commercial, and energy sectors to facilitate the widespread adoption of hydrogen. The focus is on developing methods with improved energy density and enhanced safety standards. This involves advancing technologies for storing hydrogen as a compressed gas, a cryogenic liquid, or within solid-state materials like metal hydrides and liquid organic hydrogen carriers (LOHCs), as well as utilizing geological formations like salt caverns for large-scale, long-duration storage.

Developing a robust and interconnected global hydrogen infrastructure is critical to meeting future energy demands and facilitating the widespread adoption of hydrogen as a key energy carrier. This involves not only building new pipelines, liquefaction plants, and refueling stations, but also strategically leveraging and adapting existing infrastructure where feasible. The goal is to ensure efficient and cost-effective production, storage, and distribution of hydrogen on a global scale, supporting its integration into diverse sectors from industry to transportation (Bhuiyan & Siddique, 2025).

3. **Dynamic Operation and Process Simulation:**

Given the variability of renewable energy sources, optimizing electrolyzer operation under dynamic conditions is crucial. Process simulation tools like Aspen Plus are increasingly employed to model dynamic behaviors, optimize operating strategies, and perform techno-economic assessments (Jang et al., 2021). Simulation thus supports the development of scalable and resilient green hydrogen production systems (Ren et al., 2024).

In conclusion, while green hydrogen production has made notable advances, its large-scale deployment depends on continuous technological improvements, integrated system design, and supportive policy frameworks. The integration of water electrolysis with renewable energy and the use of advanced simulation tools will be instrumental in overcoming existing barriers and unlocking the full potential of a sustainable hydrogen economy.

2.1.2 Discuss the challenges and opportunities associated with different renewable energy-powered electrolysis systems

The integration of renewable energy sources with electrolysis systems for green hydrogen (GH) production presents a dynamic landscape of both significant challenges and compelling opportunities. The specific nature of these challenges and opportunities often depends on the type of renewable energy source employed – primarily solar or wind. While renewable energy-powered electrolysis offers significant promise for green hydrogen production, several challenges must be addressed to ensure its widespread adoption.

One major technical challenge is the intermittent and fluctuating nature of renewable energy sources such as solar and wind. Electrolysis systems must be capable of operating efficiently under variable power inputs without compromising durability or efficiency. This issue is particularly relevant for alkaline electrolysis (AEL) systems, where operation under fluctuating conditions can accelerate electrode degradation and increase maintenance needs (Zeng & Zhang, 2022; Carmo et al., 2013). These challenges will be further analyzed in the simulation phase of this study, particularly focusing on alkaline electrolysis performance under dynamic renewable inputs.

Another critical barrier is the high capital cost associated with electrolyzers and renewable energy infrastructure. Current estimates place the cost of green hydrogen production between 3–6 €/kg, depending largely on electricity prices and electrolyzer efficiency (International Energy Agency [IEA], 2022; Schmidt et al., 2017). Reducing the costs of electrolyzer manufacturing is essential to making green hydrogen economically competitive.

Across both solar and wind, high upfront capital costs for electrolyzer systems, especially advanced types such as proton exchange membrane (PEM) and solid oxide electrolysis cells (SOEC), remain a barrier (Gahleitner, 2013). Effectively integrating intermittent renewable energy sources with electrolyzers requires sophisticated power electronics, control systems, and often some form of intermediate energy storage to smooth out fluctuations, adding to system

complexity (Rahman et al., 2021). Moreover, producing hydrogen is only part of the solution; cost-effective and safe methods for storing large quantities of hydrogen and distributing it to end-users are crucial and currently represent significant infrastructure gaps (Staffell et al., 2019). Finally, electrolysis requires high-purity water, which can be a concern in water-stressed regions, though research into seawater electrolysis is ongoing (Vincent et al., 2020).

Efficiency limitations also pose a challenge. Although advances have improved the performance of AEL, PEM, and SOEC technologies, the overall energy efficiency of water electrolysis remains lower compared to traditional hydrogen production methods such as steam methane reforming (Turner, 2004). Increasing the efficiency of electrolysis systems through optimized operating conditions, improved catalysts, and enhanced thermal integration is a key area of ongoing research (Rosen & Kocha, 2021).

Additionally, there are challenges related to the scale-up and integration of electrolysis plants into existing energy systems. The fluctuating nature of renewable generation necessitates advanced control strategies and robust grid management to prevent instability and ensure reliable hydrogen production (Gupta et al., 2020).

On the opportunity side, the flexibility of electrolysis systems to operate dynamically offers a valuable service to the electrical grid. They can act as flexible loads, consuming excess renewable electricity during periods of oversupply and reducing demand during shortages. This capability can significantly enhance grid stability and facilitate the integration of higher shares of renewables (Rehman et al., 2021).

Hydrogen serves as an excellent long-duration energy storage medium. Excess renewable electricity can be converted into hydrogen and stored for days, weeks, or even seasons, addressing the intermittency of renewables and complementing shorter-duration battery storage (Dutta et al., 2020). This stored hydrogen can then be reconverted to electricity via fuel cells or gas turbines during periods of low renewable output or high demand. By consuming surplus renewable energy that would otherwise be wasted, electrolyzers enable higher utilization rates of renewable assets, improving their economic viability (Jacobson et al., 2017). Furthermore, electrolyzers can act as flexible loads, adjusting their operation to absorb excess power during high renewable generation or reduce demand during grid congestion, thereby providing valuable grid balancing services (Miller et al., 2018).

Furthermore, there is a growing potential for technological synergy. For instance, coupling electrolysis with energy storage systems, such as batteries or thermal storage, can mitigate the impact of renewable intermittency (Luo et al., 2015). Similarly, the use of waste heat from industrial processes to power high-temperature electrolysis can substantially improve overall system efficiency (Hauch et al., 2015).

Producing hydrogen with zero or near-zero emissions directly contributes to climate change mitigation and helps meet global decarbonization targets (IEA, 2021). The growing demand for green hydrogen stimulates new industries, creating jobs in manufacturing, engineering, installation, and operation (IRENA, 2020). Green hydrogen also lessens dependence on fossil fuels, enhancing energy security and reducing exposure to volatile fuel prices (Díaz et al., 2022). Solar-powered electrolysis, in particular, offers the potential for decentralized hydrogen production close to the point of consumption, reducing the need for extensive new pipeline infrastructure and minimizing transmission losses (Singh et al., 2021).

Ongoing research and development are continuously driving down the cost of electrolyzers, renewable energy technologies, and hydrogen storage solutions through economies of scale, improved materials, and enhanced efficiency. Innovations in electrolyzer design, catalysts, and system integration are leading to higher conversion efficiencies for the entire renewable-to-hydrogen pathway (Turner et al., 2020). Moreover, combining solar and wind with other technologies (e.g., batteries) can create robust hybrid systems that optimize energy flow and hydrogen production, maximizing efficiency and reliability (Kondratenko et al., 2019).

Policy support and investment in research and development also present critical opportunities. Many countries have launched green hydrogen strategies that include subsidies, pilot projects, and funding for technological innovation. Such initiatives are expected to accelerate the commercialization of renewable energy-powered electrolysis systems in the coming decade (European Commission, 2020).

Overcoming these challenges through technological advancements and supportive policies will be crucial for the large-scale adoption of green hydrogen production systems. This study aims to contribute to these efforts by evaluating the performance and optimization of alkaline electrolysis under dynamic renewable energy supply conditions using Aspen Plus simulation tools.

3. Objectives and Scope

The escalating global demand for sustainable energy solutions has positioned green hydrogen as a pivotal component in the transition towards a decarbonized future. Produced through the electrolysis of water using renewable electricity, green hydrogen offers a versatile and environmentally benign energy carrier. However, the widespread adoption of this technology hinges on developing highly efficient, cost-effective, and scalable production processes.

This chapter outlines the objectives and scope of a comprehensive simulation study focused on a water electrolysis system for green hydrogen production, utilizing the powerful process simulation software, Aspen Plus. The primary aim of this research is to leverage the capabilities of Aspen Plus to design, model, and optimize a robust and efficient green hydrogen production facility. The data for the simulation of hydrogen production was adopted from work of Sánchez et al. (2020)

Specifically, the objectives of this simulation include:

a) Process Design: To establish a detailed process flowsheet for a complete water electrolysis system, encompassing all essential unit operations from water purification and electrolysis to hydrogen purification and compression.
b) Performance Evaluation: To rigorously evaluate the system's performance under various operating conditions, including temperature of feed, hydrogen production rates, energy consumption (specific energy demand), and overall system efficiency.
c) Optimization: To identify and optimize key process parameters (e.g., operating temperature, efficiency of system, and integration strategies) to maximize hydrogen yield, minimize energy intensity, and reduce operational costs.

The scope of this study will encompass:

a) Electrolysis Technology: Focusing on a specific type of water electrolysis: Alkaline Electrolysis) to ensure a focused and detailed model.
b) Ancillary Systems: Integration of essential auxiliary units, such as deionized water supply, power conditioning, gas-liquid separation, gas drying, and compression stages.
c) Energy Integration: Investigation of heat and mass integration opportunities within the process to enhance overall energy efficiency.

d) Thermodynamic Modeling: Selection and application of appropriate thermodynamic property packages within Aspen Plus to accurately predict phase equilibria and energy balances for the involved chemical species.

By achieving these objectives within the defined scope, this Aspen Plus simulation aims to provide valuable insights into the technical feasibility, operational characteristics, and optimization potential of green hydrogen production via water electrolysis, contributing to the advancement of sustainable energy technologies.

4. Methodology

This chapter outlines the comprehensive methodology employed for the simulation study of a water electrolysis system for green hydrogen production. The objective is to establish a systematic and robust framework for process design, performance evaluation, and optimization. Given the complexity and interconnectedness of chemical processes, **Aspen Plus** has been selected as the primary process simulation software due to its powerful capabilities in rigorous thermodynamic modeling, detailed unit operation simulation, and advanced optimization tools. This methodology is designed to ensure the accuracy and reliability of the simulation results, providing a strong foundation for deriving actionable insights into the technical feasibility and efficiency of the proposed green hydrogen production facility. The detail the specific steps involved will be presented, from data acquisition and model development to the application of various simulation techniques and analytical tools within the Aspen Plus environment.

4.1 System Design

The transition towards a sustainable energy future critically hinges on the effective production of green hydrogen, which necessitates a meticulously engineered system design. This subchapter provides a comprehensive overview of the proposed green hydrogen production system, detailing its architectural framework and the seamless integration of various core and auxiliary components. Here the selected electrolyzer unit will describe and discuss the inclusion of appropriate energy storage solutions where applicable. Furthermore, the design incorporates essential auxiliary components crucial for efficient and safe operation, such as gas purification, compression, and water treatment units. Each technological choice and design parameter presented herein is rigorously justified, drawing upon a thorough literature review, aligning with specific project requirements, and prioritizing sustainability considerations to ensure a robust, economically viable, and environmentally responsible hydrogen production facility.

4.1.1 Input data and assumptions

The overall structure and flow of the hydrogen production system are presented in Figure 3, which shows the simulation flowsheet developed in Aspen Plus. This diagram outlines the process layout for both the hydrogen and oxygen branches, including all major unit operations and material streams.

The data entered into the simulation are mostly based on Sánchez et al. (2020) who present modeling and experimental results for a custom model electrolyzer. These parameters are compiled in Table 1.

In the simulation, three temperature varies from 70°C, 80°C and 90°C is selected. However, the simulation steps will be shown for only one temperature. The temperature selected was 70°C, all the calculations and steps were carried out with this temperature. The steps followed for this temperature are equivalent to the others, concerning the temperature-dependent parameters.

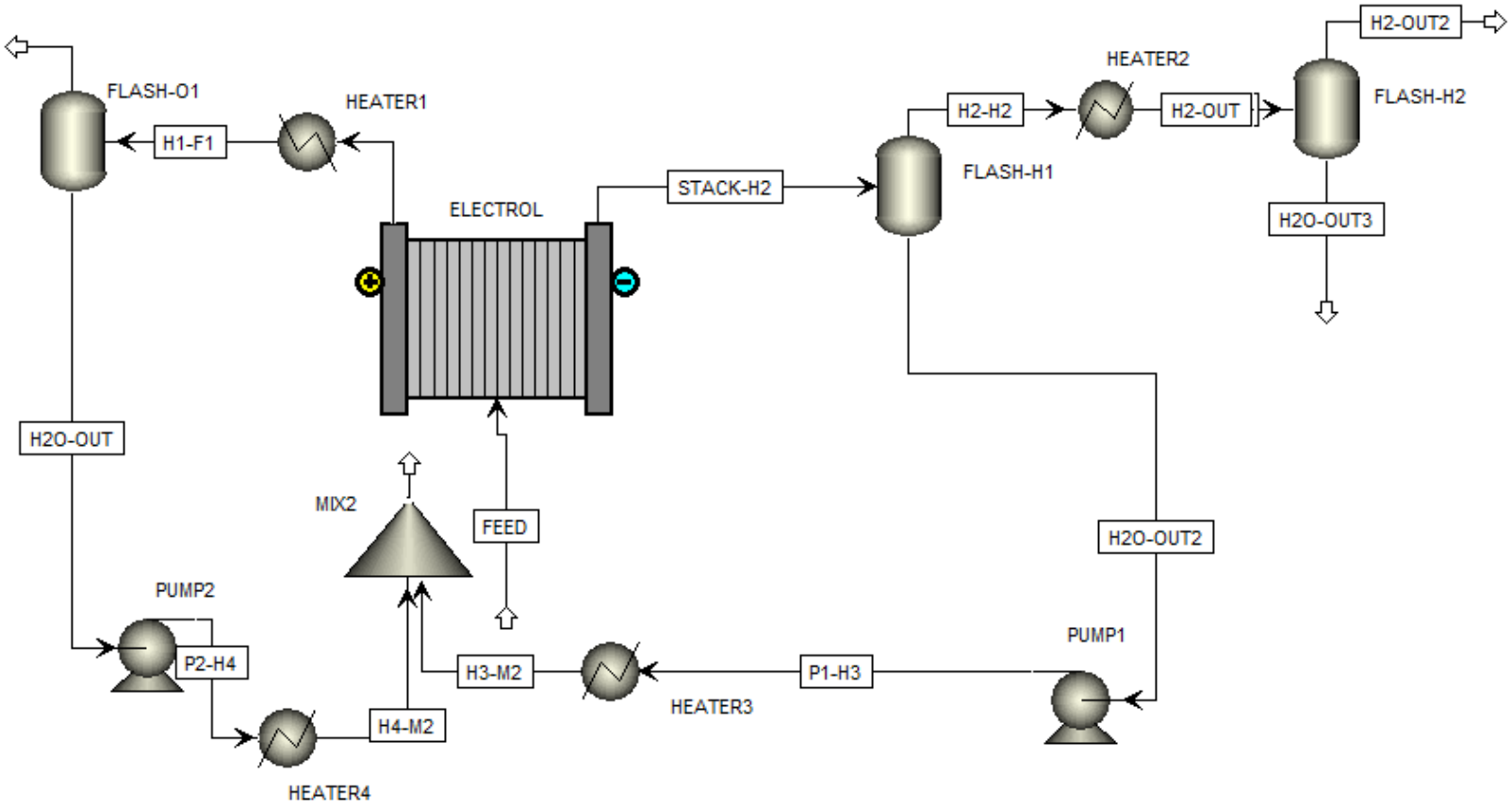

Figure 3. Scheme of the simulation flowsheet of hydrogen production

To provide clarity and systematic understanding, each piece of equipment shown in Figure 3 will be individually detailed throughout the document. For each unit, a corresponding figure will be introduced.

The depicted system is designed for hydrogen production via electrolysis, incorporating advanced stages for hydrogen purification and an extensive water recycling and conditioning loop to optimize efficiency and resource utilization.

At the heart of the system is the Electrolyzer (ELECTROL), serving as the core unit. It receives a meticulously conditioned FEED stream, which is primarily water or an aqueous solution. Within the electrolyzer, this feed is subjected to electrolysis, splitting it into two principal streams: a hydrogen-rich stream, labeled STACK-H2, and a water-rich stream, designated H2O-OUT.

The Hydrogen Purification Section processes the STACK-H2 stream from the electrolyzer. This raw hydrogen stream first enters FLASH-H1, a flash drum specifically designed to separate gaseous hydrogen from any entrained liquid water. The recovered liquid, identified as H2O-OUT2, is subsequently directed to PUMP1 for reintroduction into the system's recycling loop. The gaseous stream, primarily hydrogen (H2-H2), then undergoes further conditioning in HEATER2. This heating step is crucial for additional drying or preparing the stream for subsequent separation processes. Following heating, the stream (H2-OUT2 from HEATER2) proceeds to FLASH-H2, a second flash drum, which performs a final stage of hydrogen drying and purification. The highly purified hydrogen product ultimately exits the system as H2-OUT2 (top right outlet), while any residual separated liquid (water) is removed as H2O-OUT3.

Concurrently, the Water Recycling and Conditioning Section manages the water-rich stream (H2O-OUT) emanating from the electrolyzer, which may contain dissolved oxygen typical of water electrolysis. This stream first enters FLASH-01, where dissolved or entrained gases (such as oxygen or unreacted hydrogen) are separated and exit as FLASH-02. The liquid stream (H1-F1) from FLASH-01 is then heated by HEATER1. The heated stream subsequently enters FLASH-02, which further purifies and degasses the water, yielding another liquid outlet labeled H2O-OUT4. A primary recycled water stream, also designated H2O-OUT (originating from FLASH-02), is then pressurized by PUMP2, becoming stream P2-H4. This pressurized stream is subsequently heated by HEATER4 to form stream H4-M2. In parallel, the water recovered from the initial hydrogen purification stage (H2O-OUT2 from FLASH-H1) is pumped by PUMP1 (stream P1-H3) and subsequently heated by HEATER3 to form stream H3-M2.

Finally, these two conditioned recycle streams, H4-M2 and H3-M2, are thoroughly combined in MIX2 to create the highly conditioned FEED that is recirculated back to the electrolyzer, completing the loop and ensuring efficient resource utilization.

4.1.1.1 Feed stream

The electrolyte consists of 65 wt% water and 35 wt% KOH. This composition was selected from the data reported by Sánchez et al. (2020).

A mass flow rate of 900 kg/h was selected as a stable baseline. Higher values were tested, but they did not lead to an increase in hydrogen production. Instead, excess unreacted water remained in the system

The system was operated at a pressure of 7 bar, as reported in Sánchez et al. (2020). This pressure improves hydrogen collection efficiency and minimizes bubble formation within the system.

4.1.1.2 Electrolyzer

According to the Aspen Plus V15 Help documentation (AspenTech, 2025), the Electrolyzer Shortcut model in Aspen Plus provides a simplified approach to simulate alkaline water electrolysis processes. In alkaline electrolysis, water is split into hydrogen and oxygen using electrical energy in the presence of a liquid electrolyte, typically a concentrated potassium hydroxide (KOH) solution. The Electrolyzer Shortcut model captures the essential chemical conversion of water to hydrogen and oxygen under predefined operating conditions.

Importantly, the shortcut model calculates the overall equilibrium electrolyzer cell performance rather than simulating the detailed electrochemical phenomena such as electrode kinetics, mass transport, or ohmic losses. It assumes ideal or user-defined conversion levels and computes the product distribution accordingly. This modeling approach is visually represented in Figure 4. Electrolyzer Scheme provided by Aspen Plus.

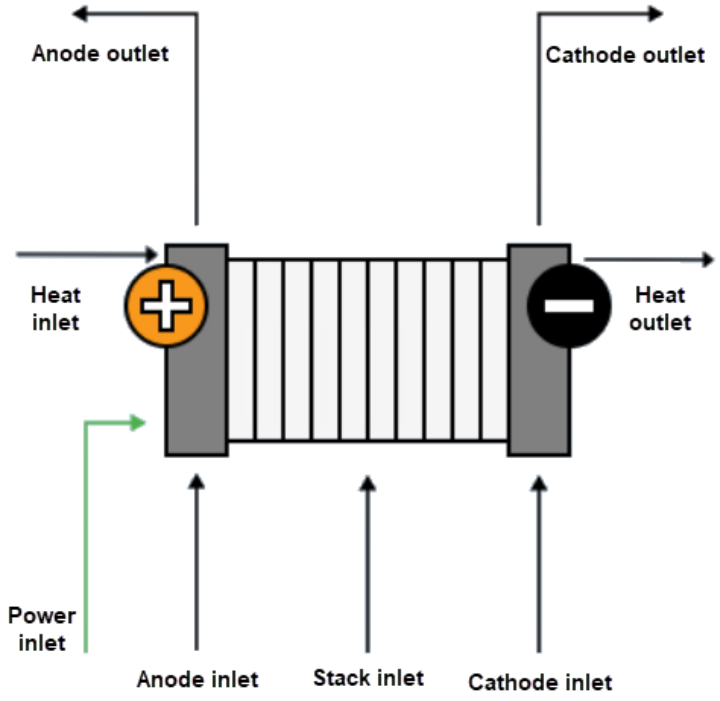

Figure 4. Electrolyzer Scheme provided by Aspen Plus

4.1.2 Alkaline Water Electrolyzer Shortcut Calculations

Electrolyzer uses the specified current or calculates it from the specified power, the specified hydrogen production rate, or the specified current density (which is current / actual area). The material balance and energy balance are based on one cell in the shortcut alkaline water electrolyzer (AspenTech, 2025).

Generation and Consumption

Electrolyzer calculates the reactions in the hydrogen production and water consumption in the cathode and the oxygen and water generation in the anode by using the following Equations 1-4.

Equation 1 calculates the molar flow rate of hydrogen generated at the cathode ($\dot{N}_{H2}^{cathode,gen}$), demonstrating its direct proportionality to the cell current (I_{cell}) and inverse proportionality to twice the Faraday constant (F_c).

$$\dot{N}_{H2}^{cathode,gen} = \frac{I_{cell}}{2F_c} \qquad (1)$$

Equation 2 determines the molar flow rate of oxygen generated at the anode ($\dot{N}_{O2}^{anode,gen}$), indicating that four times the Faraday constant is required per mole of oxygen, reflecting its production from two molecules of water.

$$\dot{N}_{O2}^{anode,gen} = \frac{I_{cell}}{4F_c} \quad (2)$$

Equation 3 shows the molar flow rate of water generated at the cathode ($\dot{N}_{H_2O}^{cathode,gen}$). This equation has the same form as the hydrogen generation rate at the cathode, suggesting a direct stoichiometric link or consideration of water as a product in that specific context.

$$\dot{N}_{H_2O}^{cathode,gen} = \frac{I_{cell}}{2F_c} \quad (3)$$

Equation 4 provides the molar flow rate of water consumed at the cathode ($\dot{N}_{H_2O}^{cathode,cons}$). This highlights the reactant role of water at the cathode side, with its consumption rate directly proportional to the cell current and inversely proportional to the Faraday constant.

$$\dot{N}_{H_2O}^{cathode,cons} = \frac{I_{cell}}{F_c} \quad (4)$$

where:

- $\dot{N}$ – Molar flow of species produced or consumed [mol/s]
- $\varepsilon_{Faraday}$ – Faradic efficiency
- I_{cell} – Current [A]
- F_c – Faraday constant [C/mol]

Total production/generation/consumption rates are obtained by multiplying by the number of cells.

Efficiency

The efficiency of the electrolyzer, a critical performance indicator, can be expressed using various metrics, as defined by the following equations Equation 5–7.

Equation 5 presents the Higher Heating Value (HHV) efficiency (ε_{HHV}). This metric relates the total energy content of the produced hydrogen (based on its HHV, H_o, and volumetric flow rate, $\tilde{V}_{H2}$) to the electrical power (P_{el}) consumed by the electrolyzer.

$$\varepsilon_{HHV} = \frac{(\tilde{V}_{H2} * H_o)}{P_{el}} \quad (5)$$

Equation 6 defines the Lower Heating Value (LHV) efficiency (ε_{LHV}). Similar to HHV efficiency, this metric uses the LHV of hydrogen (H_u) to calculate the energy output, providing an alternative perspective on efficiency, particularly relevant when the latent heat of water vapor is not recovered.

$$\varepsilon_{LHV} = \frac{(\tilde{V}_{H2} * H_u)}{P_{el}} \quad (6)$$

Equation 7 quantifies the Voltage efficiency ($\varepsilon_{Voltage}$). This efficiency is determined by the ratio of the thermoneutral voltage (E_{th}), which represents the minimum theoretical voltage required to sustain the electrolysis reaction, to the actual operating cell voltage (E_{cell}). It highlights how effectively the electrical energy supplied is converted into chemical energy of hydrogen, indicating voltage losses within the cell.

$$\varepsilon_{Voltage} = \frac{E_{th}}{E_{cell}} \quad (7)$$

where

- $\dot{V}_{H2}$ – Volumetric flow rate of hydrogen [m³/s]
- H_o – Specific high heating value of hydrogen [J/m³]
- H_u – Specific low heating value of hydrogen [J/m³]
- P_{el} – Total power of the electrolyzer [W]
- E_{cell} – Cell voltage = cell power divided by cell current [V]
- E_{th} – Thermoneutral voltage [V]

In the shortcut model, one of these efficiencies is specified.

Crossing Over of Species

Crossing over of species is modeled using one of two shortcut methods requiring one parameter specified for each of water and hydrogen.

If the water method is Fraction of unreacted H_2O crossing over, the flow rate is calculated as:

$$\dot{N}_{H_20}^{cross} = f_{H_2O} \cdot \dot{N}_{H_2O}^{unreacted} \quad (8)$$

where f_{H2O} is the fraction of water crossing over.

If the water method is Water permeation coefficient, the flow rate is calculated using the expression for osmotic dragging, as this mechanism is dominant over diffusion and pressure gradient. The dimensionless crossover coefficient can be calibrated to account for all three mechanisms to obtain a result with quality close to the rigorous model. Equation 9 is:

$$\dot{N}_{H_2O}^{cross} = C_{H_2O}^{cross-over} \cdot \frac{I_{cell}}{F_c} \quad (9)$$

C is the dimensionless crossover coefficient, I_{cell} is the cell current in amperes, and F_c is the Faraday constant in A·s/kmol.

If the hydrogen method is Fraction of total H_2 crossing over, then the flow rate is calculated by Equation 10:

$$\dot{N}_{H_2}^{cross} = f_{H_2} \cdot \dot{N}_{H_2}^{gen} \quad (10)$$

where f_{H_2} is the fraction of hydrogen crossing over.

If the hydrogen method is Hydrogen permeation constant, an expression based on the pressure gradient is used, as this is the main mechanism for hydrogen permeation. The expression uses a permeation constant based on some of the membrane parameters and the temperature, and is calculated as:

$$K_{H_2}^{permeation} = \frac{A_{membrane} \cdot D_H \cdot p_{ref}}{\delta_{membrane} \cdot R \cdot T_{cell}} \quad (11)$$

where $A_{membrane}$ is the active membrane area in m_2, D_H is the diffusion coefficient of hydrogen in m^2/s, $\delta_{membrane}$ is the membrane thickness in m, R is the gas constant in

m^2·Pa/(kmol·K), T_{cell} is the cell temperature in K, and p_{ref} is the reference pressure (101325 Pa). In this case the hydrogen crossing over is calculated as:

$$\dot{N}_{H_2}^{cross} = \left(\frac{K_{H_2}^{permeation}}{p_{ref}} \right) \cdot \left(p_{H_2}^{cathode} - p_{H_2}^{anode} \right) \quad (12)$$

Specifications

In the simulation, three different numbers of cells were tested: 12, 40 and 80 cells per stack for each value of the temperature, resulting in a total of nine different cases. For the calculations and simulation presented, 12 cells per stack were used.

A power of 10 kW was adopted directly from Sánchez et al. (2020), corresponding to the laboratory-scale system simulated in their study. Faraday efficiency and cell voltage were calculated using empirical correlations provided by the same authors (Sánchez et al. 2020), dependent on current density, temperature, and pressure.

Faraday efficiency

Equation 13 is an empirical formula used to model the Faraday efficiency (η_F) of an electrochemical system, as proposed by Sánchez et al. (2020).

$$\eta_F = \left(\frac{i^2}{f^{11} + f^{12} \cdot T + i^2} \right) \cdot \left(f^{21} + f^{22} \cdot T \right) \quad (13)$$

where:

- i – current density [A]
- T – temperature [°C]
- $f_{11}, f_{12}, f_{21}, f_{22}$ – fitted coefficients. Units of the coefficients are placed in Table 1.

Efficiency values were taken directly from interpolated data at the three temperatures studied. The coefficients provided by Sánchez et al. (2020) and used in the calculations can be found in Table 1.

Table 1. Coefficients considered for the electrochemical model (Sánchez et al. 2020)

Model	Coefficient	Value	Unit
Polarization Curve	r1	4.452×10^{-5}	$\Omega \cdot m^2$
	r2	6.888×10^{-9}	$\Omega \cdot m^2 \cdot °C^{-1}$
	d1	-3.130×10^{-6}	$\Omega \cdot m^2$
	d2	4.471×10^{-7}	$\Omega \cdot m^2 \cdot bar^{-1}$
	s	3.382×10^{-1}	V
	t1	-1.540×10^{-2}	$m^2 \cdot A^{-1}$
	t2	2.002×10^{0}	$m^2 \cdot °C \cdot A^{-1}$
	t3	1.524×10^{1}	$m^2 \cdot °C^2 \cdot A^{-1}$
Faraday efficiency	f11	4.786×10^{5}	$A^2 \cdot m^{-4}$
	f12	-2.953×10^{3}	$A^2 \cdot m^{-4} \cdot °C^{-1}$
	f21	1.040×10^{0}	-
	f22	-1.004×10^{-3}	$°C^{-1}$
Gas purity (H_2 in O_2)	C1	9.901×10^{-2}	-
	C2	-2.007×10^{-3}	$°C^{-1}$
	C3	1.310×10^{-5}	$°C^{-2}$
	C4	-8.484×10^{-2}	-
	C5	1.790×10^{-3}	$°C^{-1}$
	C6	-1.133×10^{-5}	$°C^{-2}$
	C7	1.481×10^{3}	$A \cdot m^{-2}$
	C8	-2.360×10^{1}	$A \cdot m^{-2} \cdot °C^{-1}$
	C9	-2.577×10^{-1}	$A \cdot m^{-2} \cdot °C^{-2}$
	E1	3.714×10^{0}	-
	E2	-9.306×10^{-1}	bar^{-1}
	E3	5.817×10^{-2}	bar^{-2}
	E4	-3.721×10^{0}	-
	E5	9.321×10^{-1}	bar^{-1}
	E6	-5.826×10^{-2}	bar^{-2}
	E7	-1.838×10^{1}	$A \cdot m^{-2}$
	E8	5.873×10^{0}	$A \cdot m^{-2} \cdot bar^{-1}$
	E9	-4.625×10^{-1}	$A \cdot m^{-2} \cdot bar^{-2}$

Voltage efficiency

Voltage efficiency (η) is an essential parameter for evaluating the performance of an electrolyzer, as it indicates how efficiently electrical energy is converted into chemical energy under practical operating conditions. It is defined as the ratio between the reversible voltage V_{rev} and the actual cell voltage V_{cell}, as shown in the Equation 14:

$$\eta = \frac{V_{rev}}{V_{cell}} \quad (14)$$

This efficiency can be interpreted as a specific form of exergy efficiency, representing how far the real electrochemical process deviates from the ideal, thermodynamically reversible condition. For the hydrogen and oxygen reaction at standard conditions forming liquid water, the reversible cell voltage is approximately 1.229 V (Li, 2007).

Also, from Sánchez et al. (2020), the voltage efficiency was defined and applied to determine the actual cell voltage used in energy calculations, by adapting Equation 15.

$$V_{cell} = V_{rev} + [(r_1 + d_1) + r_2 * T + d_2 * p] * i + s * log\left[\left(t_1 + \frac{t_2}{T} + \frac{t_3}{T^2}\right) * i + 1\right] \quad (15)$$

The coefficients provided by Sánchez et al. (2020) and used in the calculations can be found in **¡Error! No se encuentra el origen de la referencia.**Table 1**.**

Hydrogen Permeation

Hydrogen solubility represents the equilibrium concentration of dissolved hydrogen gas within the membrane material under specific pressure and temperature conditions.

Hydrogen diffusion describes the kinetic process by which hydrogen molecules move through the membrane material under concentration gradients. Unlike solubility, diffusion is highly sensitive to temperature and follows Arrhenius-type behavior due to the thermally activated nature of molecular transport.

Permeation is the complete process where hydrogen passes through a material, combining solubility and diffusion. It includes absorption at one surface, diffusion through the material, and desorption at the opposite surface. Permeation rate depends on both how well the material can dissolve hydrogen and how quickly it can move through it.

The permeation constant quantifies how easily hydrogen traverses a material. It is the product of solubility and diffusion coefficient. Materials with high permeation constants allow rapid hydrogen passage, while those with low constants act as effective barriers (Barbir, 2013).

4.1.3 Hydrogen Branch

After the electrolysis process, the hydrogen exiting the cell is mixed with unreacted water and potassium hydroxide (KOH). To achieve high hydrogen purity, a two-stage purification system is employed. In Flash 1, the majority of the liquid-phase water and KOH is separated

from the gas stream. The gas then passes through a cooler, which reduces its temperature to 25 °C and it is depressurized to 5 bar. Then, the stream enters Flash 2, where the remaining water vapor is removed. The resulting purified hydrogen is then directed to storage tanks. At the same time, the liquid collected in Flash 1, referred to as stream H_2O-OUT2, is pumped, reheated, and recirculated into the feed stream. This internal recirculation process can improve the system's sustainability by lowering freshwater consumption and minimizing waste generation. However, this full integration led to numerical errors within the simulation environment, preventing the convergence of results. A notable issue encountered was the erroneous appearance of oxygen (O2) in the purified hydrogen (H2) stream, which is physically implausible under normal operating conditions and indicative of computational instability. Despite these challenges with the complete recirculation setup, successful simulation results were obtained for a simplified configuration involving only one circulation loop but not connected with feed stream. This allowed for a focused investigation where the flow returning from the oxygen-rich water loop was analyzed separately from the flow returning from the hydrogen purification loop, providing valuable insights into individual recycling stream behaviors and their impact on the overall system performance. This iterative approach to simulation helped in identifying areas of complexity and potential numerical sensitivities within the integrated system. The simulation flowsheet with the complete recirculation loop will be further explained in this subchapter.

4.1.4 Oxygen Branch

On the anodic side, oxygen exits the electrolyzer along with unreacted water and KOH. The mixture is first cooled to 25°C and depressurized to 5 bar, ensuring that water vapor condenses. A subsequent Flash 3 unit separates the liquid from gaseous oxygen. The oxygen stream is stored, while the liquid is pumped and reheated for reuse with the feed. As noted above, the full recirculation loop encountered operational issues. As in the hydrogen branch, recirculation plays a key role in resource conservation and process efficiency.

4.2 Develop a detailed Aspen Plus model

This subchapter presents a comprehensive development of the Aspen Plus simulation model used to represent the alkaline water electrolysis process. Each unit operation included in the model is described in detail, focusing on its specific role, operating conditions, and configuration within the process. The operating parameters—such as temperature, pressure, and composition—have been carefully selected based on technical literature, experimental data, or

rational engineering assumptions. The methodology followed for estimating and justifying these input values will be thoroughly explained to ensure transparency and reproducibility.

To maintain clarity and logical flow, the explanation will follow the layout of the simulation flowsheet of hydrogen production shown in Figure 3, proceeding step by step through the process. This approach not only facilitates a better understanding of how each unit contributes to the overall system performance but also highlights the integration and interaction among the different process components. This process flow diagram (Figure 3) illustrates a system primarily focused on hydrogen production via electrolysis, with a comprehensive water recycling and conditioning system. The main components and the overall process flow: Electrolyzer (ELECTROL); hydrogen purification section (Right Side): separators FLASH-H1 and FLASH-H2, heat exchanger HEATER2 and HEATER3; pump PUMP1; water recycling and conditioning section (Left and Bottom Side): separators: FLASH-01 and FLASH-02; heat exchanger HEATER1 and HEATER4; pump PUMP2 and mixer: MIX2.

The objective of this section is to provide a clear and precise understanding of how the simulation was constructed, how the data was selected, and how the virtual representation reflects the real behavior of the electrolysis system under study.

1. **Feed input stream configuration**

The feed stream entering the electrolysis system is configured with specific thermodynamic and composition parameters, as is presented in Figure 5. The solution described is a typical alkaline electrolyte, commonly used in methods for hydrogen production, such as alkaline water electrolysis. The stream operates at a temperature of 70°C and a pressure of 7 bar, with a total mass flow rate of 900 kg/hr. The feed composition consists of 65% water (H2O) and 35% potassium hydroxide (KOH) by mass fraction, representing a typical alkaline electrolyte solution. The values of pressure and feed composition were obtained from Sánchez et al. (2020). The remaining components are initially set to zero, indicating a pure electrolyte feed without dissolved gases or additional ionic species.

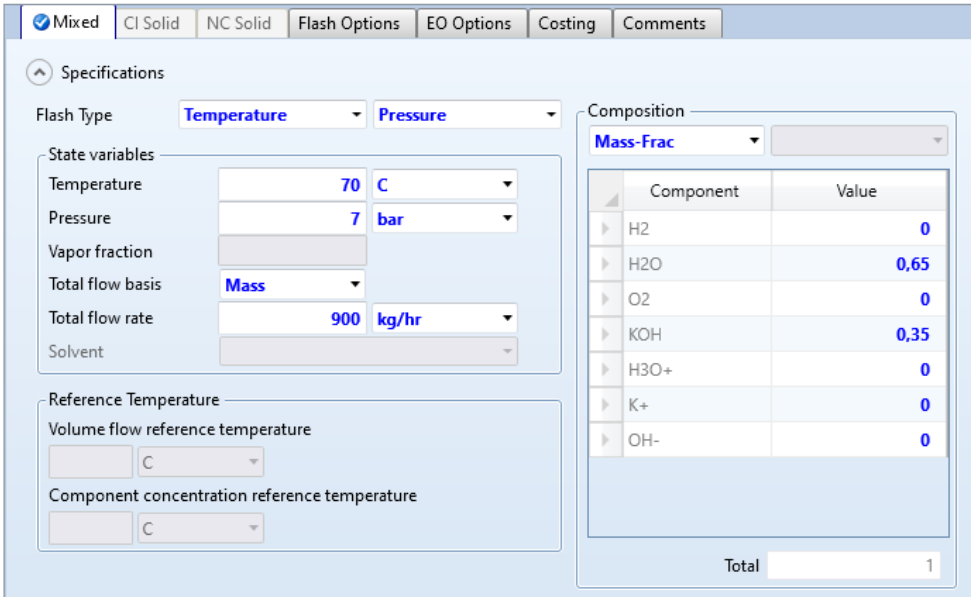

Figure 5. Feed Stream Specifications and Composition Configuration

2. Electrolyzer Unit Specifications

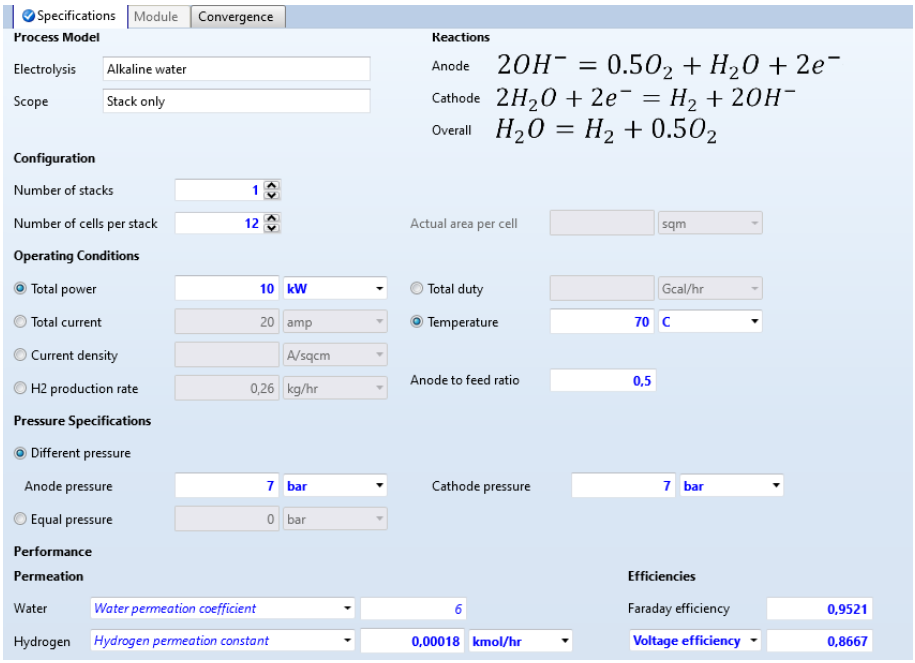

Figure 6. Electrolyzer Unit Configuration and Operating Parameters

The electrolyzer is modeled as an alkaline water electrolysis system operating under controlled conditions, as shown in Figure 6. The unit configuration includes a single stack containing 12 individual cells, designed to operate at a total power consumption of 10 kW. The operating temperature is maintained at 70°C with both anode and cathode pressures set to 7 bar, ensuring consistent operating conditions throughout the electrochemical process.

The electrochemical reactions are defined for the alkaline water electrolysis process as follows:

Anode reaction: $2OH^- \rightarrow 0.5O_2 + H_2O + 2e^-$

Cathode reaction: $2H_2O + 2e^- \rightarrow H_2 + 2OH^-$

Overall reaction: $H_2O \rightarrow H_2 + 0.5O_2$

The anode reaction involves the oxidation of hydroxide ions to produce oxygen gas, water, and electrons, while the cathode reaction generates hydrogen gas through the reduction of water molecules, consuming electrons and producing hydroxide ions. The overall process represents the electrochemical decomposition of water into its constituent gases.

The system performance is characterized by high operational efficiencies, with a Faraday efficiency of 95.21% calculated using Equation 13, indicating excellent current utilization for the electrochemical reaction, and a voltage efficiency of 86.67% determined through Equations 14 and 15, representing good energy conversion performance. The anode to feed ratio is configured at 0.5, optimizing the distribution of reactants between the electrode compartments.

3. Hydrogen Branch

Flash-H1

The product stream from the electrolyzer undergoes a two-stage flash separation process for gas-liquid separation and product purification. The first flash separator (Flash 1) operates at 70°C and 5 bar, maintaining the electrolyzer operating temperature while reducing the pressure to facilitate initial phase separation between the gaseous products and the liquid electrolyte solution, as illustrated in Figure 7.

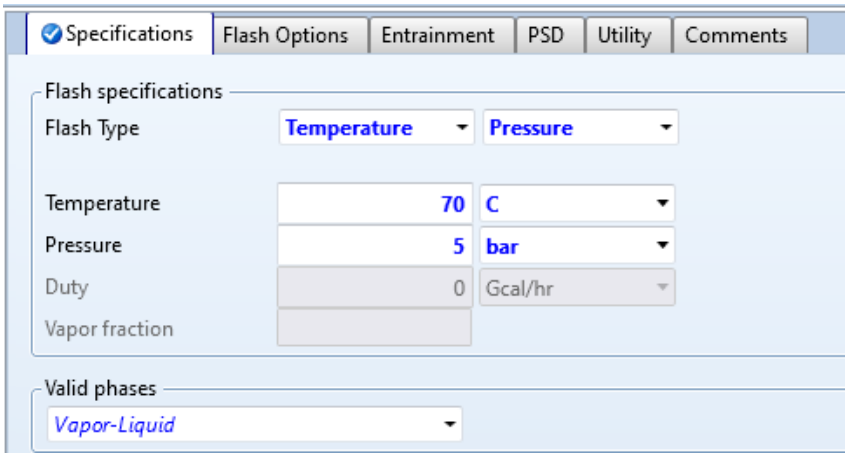

Figure 7. Flash Separator 1 - Initial Gas-Liquid Separation Specifications

HEATER2 (COOLER OF HYDROGEN)

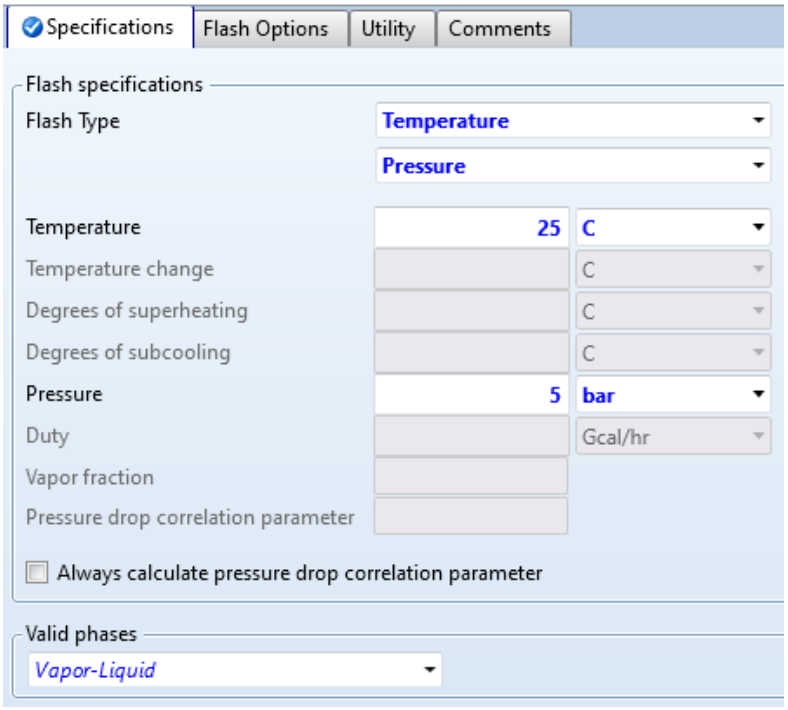

Figure 8. Cooling Unit Specifications - Hydrogen Stream Temperature Reduction

Following the first separation stage, the stream is processed through a second flash separator (Flash 2) operating at reduced conditions of 25°C and 5 bar in cooler (HEATER2). This temperature reduction from 70°C to 25°C indicates the presence of an intermediate cooling step between the flash units, as shown in Figure 8, which enhances the separation efficiency and allows for better hydrogen purification by condensing water vapor and improving the phase equilibrium conditions.

Both flash separators are configured for vapor-liquid equilibrium calculations, ensuring accurate prediction of the gas-liquid distribution and optimal separation performance for the hydrogen recovery process, with Flash 2 results demonstrated in Figure 9.

FLASH H2

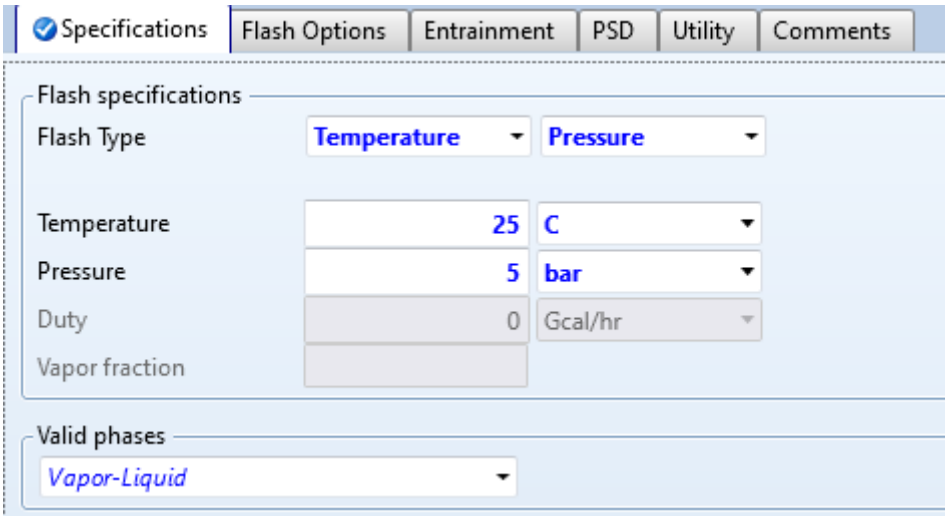

Figure 9. Flash Separator 2 - Final Hydrogen Purification Unit Configuration

PUMP 1 (H2 RECIRCULATE)

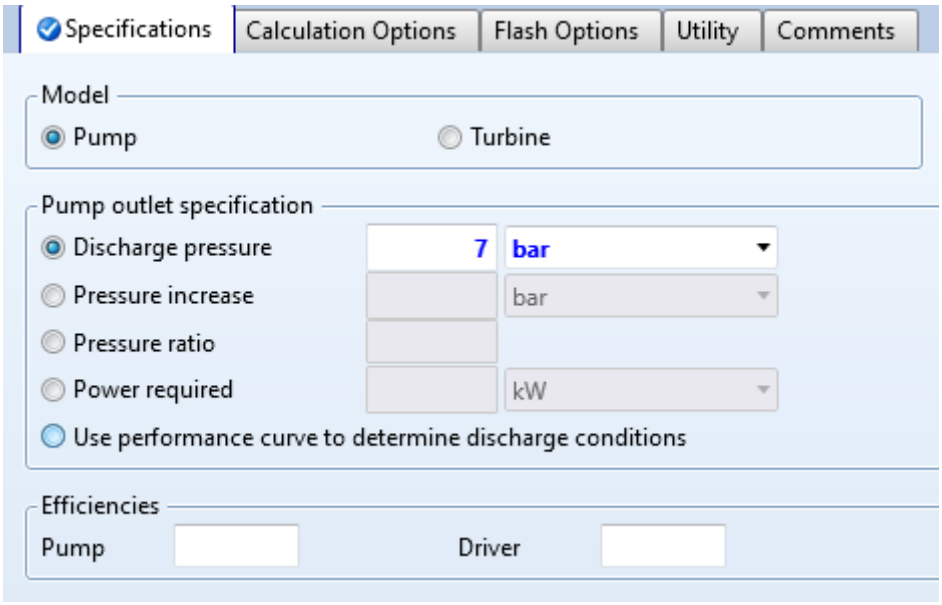

Figure 10. Electrolyte Recycle Pump Specifications - Hydrogen Branch Water Recovery

Following the initial flash separation, the hydrogen-rich stream undergoes further processing through a dedicated compression and heating system. A centrifugal pump is employed to increase the hydrogen stream pressure from the flash separator outlet to the required system pressure of 7 bar. The pump is configured with a discharge pressure specification, utilizing performance curves to determine optimal discharge conditions while maintaining appropriate pump and driver efficiencies, as illustrated in Figure 10.

HEATER 3 (HEAT RECIRCULATE H2)

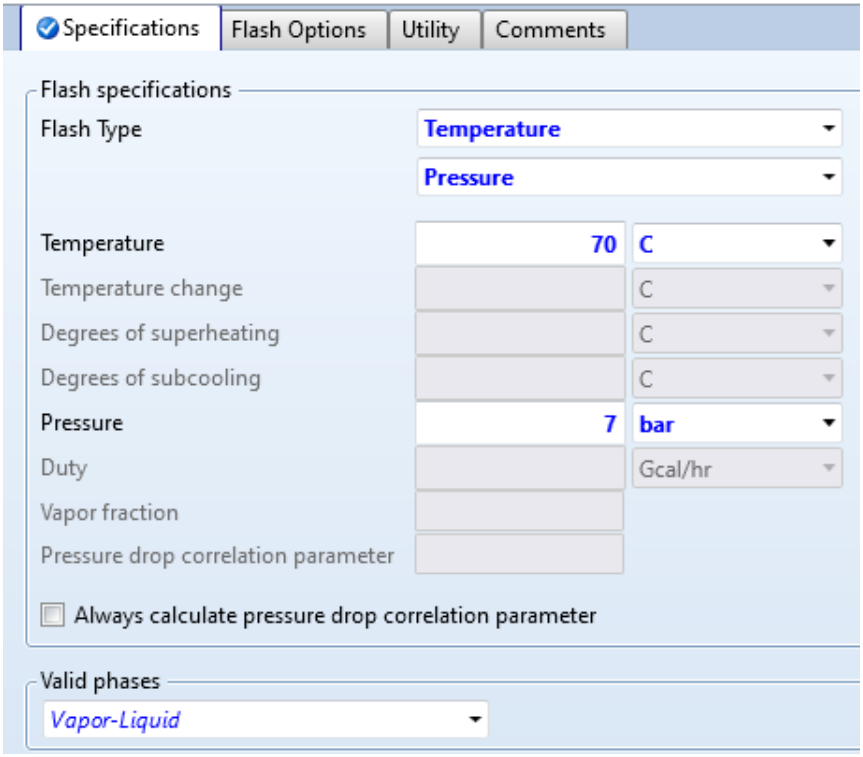

Figure 11. Electrolyte Recycle Heater Specifications - Hydrogen Branch Water Recovery

The compressed hydrogen stream is then processed through a heating unit (HEATER2) designed to condition the gas temperature for downstream operations. This heating step ensures optimal temperature conditions for the subsequent flash separation stage (FLASH-H2), which operates at 70°C and 7 bar, maintaining vapor-liquid equilibrium for final hydrogen purification and moisture removal. The heating system and flash separation results are presented in Figure 11.

4. Oxygen Branch

COOLER 1 (O2)

As depicted in Figure 12, the oxygen-rich stream from the electrolyzer follows a parallel processing path designed for oxygen recovery and conditioning. The stream initially passes through a cooling system (HEATER3) to reduce the temperature from the electrolyzer operating conditions to 25°C, facilitating improved phase separation and oxygen recovery in the subsequent flash unit.

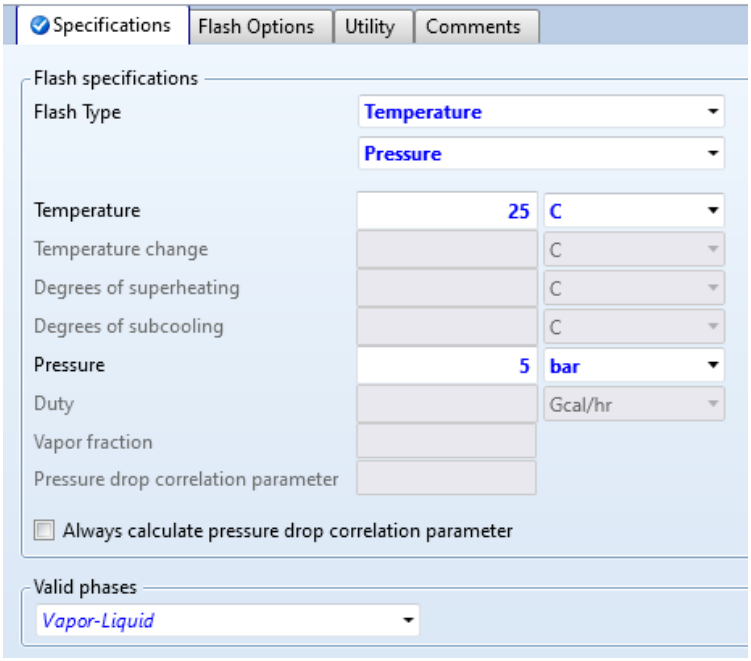

Figure 12. Oxygen Stream Cooling Unit Specifications

FLASH O1

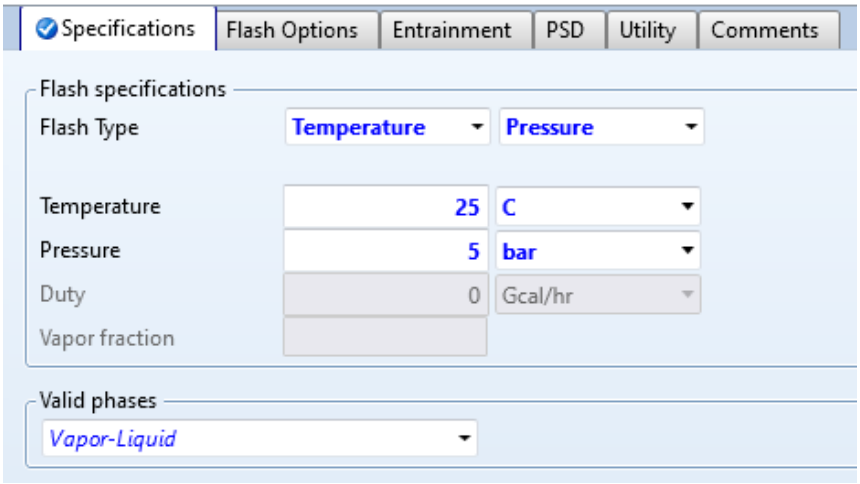

Figure 13. Flash Unit Configuration for Oxygen Purification

As shown in Figure 13, the cooled oxygen stream enters a flash separator (FLASH-H1) operating at 25°C and 5 bar, configured for vapor-liquid separation to remove residual water and electrolyte components from the oxygen product. This separation produces two distinct streams: the purified oxygen vapor phase, which is directed to storage tanks as the final oxygen product, and the liquid phase containing the remaining water and KOH electrolyte.

PUMP 2

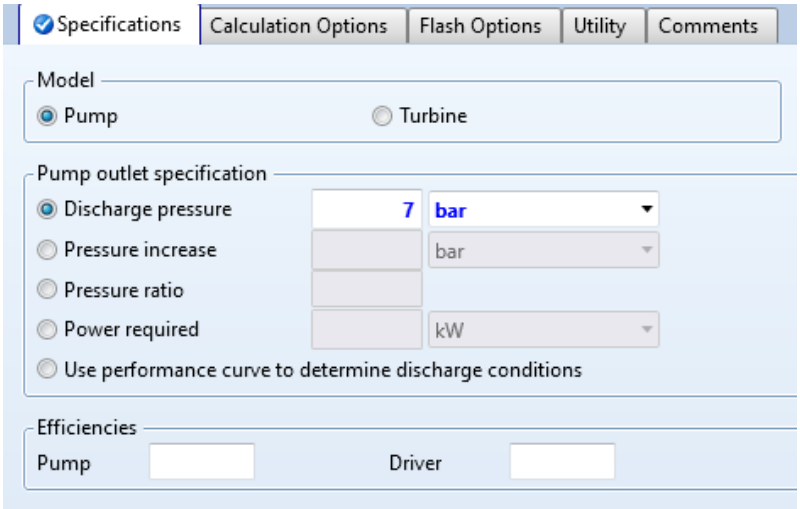

Figure 14. Electrolyte Recycle Pump Specifications - Oxygen Branch Water Recovery

The liquid phase from the flash separator, rich in water and potassium hydroxide electrolyte, undergoes a recycle processing sequence to maximize electrolyte recovery and system efficiency. The configuration presented in Figure 14 shows this aqueous electrolyte stream is first compressed using a centrifugal pump (PUMP2) with a discharge pressure specification of 7 bar to match the feed system pressure requirements.

HEATER 4

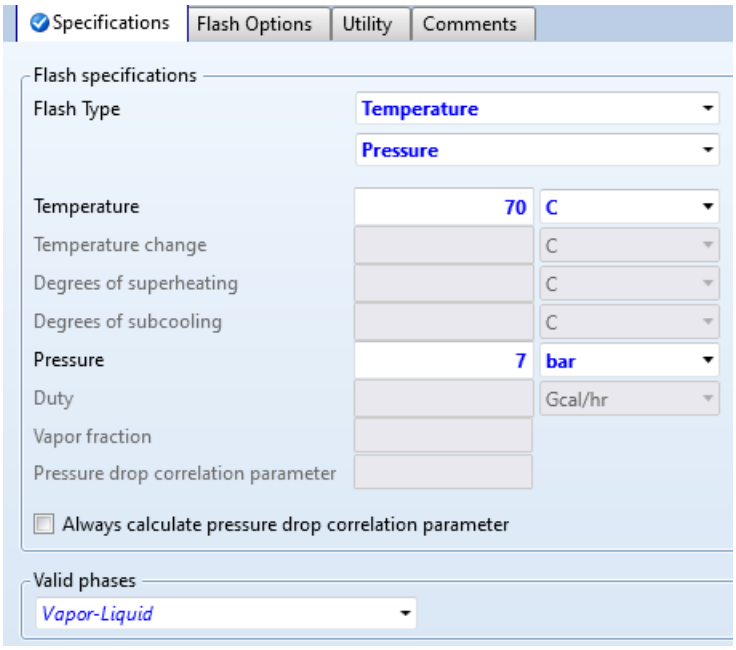

Figure 15. Electrolyte Recycle Heater Specifications - Oxygen Branch Water Recovery

Figure 15 shows the compressed liquid stream is subsequently heated through a heating unit (HEATER4) to bring the temperature back to 70°C, matching the electrolyzer operating.

MIXER

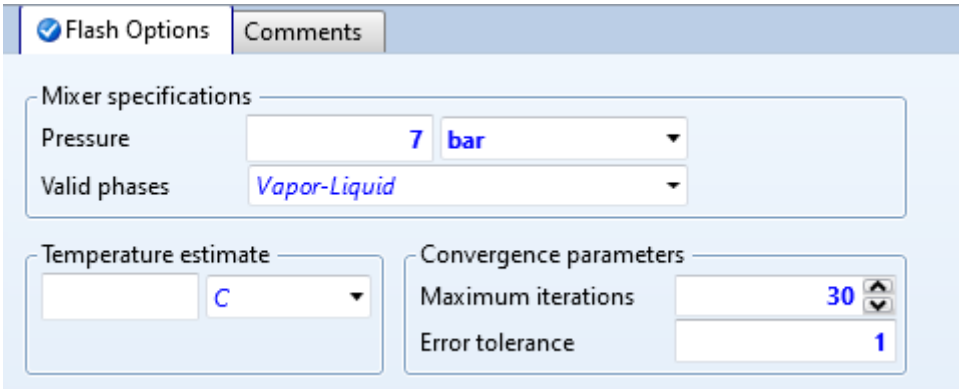

Figure 16. Electrolyte Recycle Mixer - Configuration and Convergence Parameters

As demonstrated in Figure 16**,** the conditioned electrolyte recycle stream is then combined with the liquid waste stream from the hydrogen processing branch in a mixer unit (MIX2) operating at 7 bar with vapor-liquid phase equilibrium. This mixing operation consolidates both liquid waste streams containing water and KOH electrolyte from both the hydrogen and oxygen separation processes, allowing for the recovery and reuse of the valuable electrolyte components while maintaining the required water-to-electrolyte ratio for optimal electrolyzer performance. The mixer is configured with convergence parameters including a maximum of 30 iterations and an error tolerance of 1, ensuring accurate material and energy balance calculations for the combined stream entering the electrolysis system.

5.0 Results and Discussion

This chapter presents the comprehensive analysis of the alkaline water electrolysis system modeled in Aspen Plus, focusing on the performance evaluation under different operating conditions and system configurations. The results are structured into two main parts to provide a systematic comparison of system performance and design alternatives.

Part I: Simulation without Circulation Loop - This section analyzes the basic electrolysis system where the liquid streams from the flash separators are not recycled back to the feed. This configuration represents a simplified process that allows for the evaluation of fundamental electrolyzer performance without the complexity of material recirculation. The analysis focuses on hydrogen production rates, energy efficiencies, and material consumption under various operating conditions.

Part II: Simulation with Circulation Loop - This section examines the complete integrated system where the KOH electrolyte and water recovered from the hydrogen and oxygen separation processes are recycled back to the electrolyzer feed. This configuration represents a more realistic and sustainable industrial process that minimizes waste generation and maximizes resource utilization. However, during the simulation, numerical errors prevented the successful convergence of the circulation loop

The comparative analysis between both configurations provides valuable insights into:

- Resource Efficiency: Water consumption, electrolyte utilization, and waste generation
- Energy Performance: Total energy requirements including auxiliary equipment for recirculation
- Operational Complexity: Trade-offs between process efficiency and system complexity

All simulation results are compared systematically to identify the optimal operating conditions and to quantify the benefits of implementing electrolyte recirculation. The analysis considers multiple performance metrics including hydrogen production rates, specific energy consumption (kWh/kg H_2), Faraday efficiency, voltage efficiency, and overall system efficiency. Additionally, the environmental impact of each configuration is evaluated in terms of water consumption and waste generation.

In order to compare the obtained modeling results, identical electrolyzer operating conditions (temperature, pressure, power input) were used to isolate the effects of the recirculation system on overall process performance. This approach provides a clear

understanding of the value proposition for implementing circulation loops in alkaline water electrolysis systems for industrial hydrogen production.

5.1 Part I: Simulation without Circulation Loop

The developed Aspen Plus model was validated against experimental data from Sánchez et al. (2020), who presented both modeling and experimental results for a custom alkaline electrolyzer. The validation process focused on key performance indicators including Faraday efficiency, voltage efficiency, and hydrogen production rates under comparable operating conditions.

5.1.1 Faraday Efficiency Validation

The Faraday efficiency was calculated using the empirical correlation provided by Sánchez et al. (2020) using Equation 13.

The coefficients used in the calculation were obtained from the experimental data provided by Sánchez et al. (2020), which includes the following parameters:

$f_{11} = 4.786 \times 10^{5}\ A^2 \cdot m^{-4}$

$f_{12} = -2.953 \times 10^{3}\ A^2 \cdot m^{-4} \cdot °C^{-1}$

$f_{21} = 1.040$

$f_{22} = -1.004 \times 10^{-3}\ °C^{-1}$

Using these experimentally derived coefficients, the simulation achieved a Faraday efficiency of 95.21% at 70°C and 7 bar operating conditions. This high efficiency indicates excellent current utilization for the electrochemical reaction and demonstrates that the model accurately reproduces the experimental behavior reported in the reference study.

4.1.2 Voltage Efficiency Analysis

The voltage efficiency was calculated using Equation 14.

Where the cell voltage is determined by the polarization curve equation from Sánchez et al. (2020) with Equation 15.

Applying the experimental coefficients provided by Sánchez et al. (2020), the simulation achieved a voltage efficiency of 86.67% at 70°C and 7 bar operating conditions. This value demonstrates excellent energy conversion performance, indicating that the electrochemical

system is highly efficient in converting electrical energy into the desired chemical product, with minimal energy losses to heat. Such high efficiency is crucial for the economic viability and sustainability of industrial processes, as it directly translates to reduced electricity consumption and lower operating costs. Furthermore, this achieved efficiency is highly consistent with the experimental data reported in the reference study for similar operating conditions, thereby validating the accuracy of the simulation model and the applicability of the coefficients derived. The favorable operating temperature of 70°C likely contributes positively by enhancing reaction kinetics and reducing ohmic resistance, while the pressure of 7 bar might play a role in optimizing gas-liquid interfaces and product removal, collectively leading to this robust performance.

5.1.3 Results of Electrolyzer

This subchapter presents the main simulation results obtained for the electrolyzer system under various operating conditions. The primary objective of this analysis was to thoroughly investigate the impact of two critical operational and design parameters on the electrolyzer's performance: the number of cells per stack and the operating temperature.

To achieve a comprehensive understanding, a structured simulation matrix was developed, comprising a total of nine distinct cases. These cases were created by systematically combining three different cell stack configurations (12, 40, and 80 cells per stack) with three representative operating temperatures (70°C, 80°C, and 90°C). This systematic approach allowed for a robust evaluation of how scaling the number of cells and varying thermal conditions influence the system’s output and efficiency.

Crucially, all simulations were consistently run under controlled conditions to isolate the effects of the chosen parameters. Specifically, a fixed operating pressure of 7 bar was maintained across all cases, ensuring that pressure-related variables did not confound the analysis. Similarly, a constant input power of 10 kW was supplied to the electrolyzer system for every simulation run. This standardized input power enabled a direct comparison of energy conversion performance and product output across the different cell configurations and temperatures, providing clear insights into the optimal operating windows for this specific electrolyzer design. The main results obtained from the comprehensive electrolyzer model simulations are systematically presented in Table 2, Table 3, Table 4. These tables summarize the key performance indicators derived from combining various cell stack configurations and operating temperatures under constant pressure and input power.

Upon initial examination of these results, several significant trends and relationships become apparent. Firstly, it consistently observes that increasing the operating temperature generally leads to an improvement in the overall voltage efficiency of the electrolyzer. This is a well-established electrochemical principle, as higher temperatures enhance reaction kinetics, reduce activation overpotentials, and improve the conductivity of the electrolyte, thereby minimizing energy losses. Conversely, the specific energy consumption (e.g., in kWh per kg of hydrogen produced) tends to decrease with rising temperature, highlighting the energy benefits of operating at elevated temperatures within the tested range.

It can be observed that in Tables 3–5, the hydrogen production rate, oxygen production rate, and water consumption rate remain constant regardless of the number of cells. This behavior might seem counterintuitive at first glance, however, it is consistent with the theoretical formulation used in the model. The number of cells per stack plays a crucial role in shaping the electrolyzer's performance characteristics. As the number of cells in the stack increases from 12 to 80, while maintaining a fixed total input power of 10 kW, the current density across individual cells necessarily decreases. This reduction in current density per cell typically results in a lower overall cell voltage for the stack and, consequently, a higher voltage efficiency. This is primarily because ohmic and concentration overpotentials, which are highly dependent on current density, are mitigated at lower operating current densities per cell.

These values correspond to rates per cell and are calculated using Equations 1 through 4, which are based on Faraday’s law and define the molar or mass flow rate per unit of current. In the shortcut electrolyzer model used, the total current is automatically adjusted to maintain constant power (10 kW), and the calculated rates are given per single cell. Therefore, although the total current decreases when the number of cells increases (since voltage increases accordingly), the production rate per cell remains essentially the same.

To compute the total hydrogen generation, oxygen generation, or water consumption for the whole system, the values shown in Tables 2–4 must be multiplied by the number of cells. This clarifies why the reported rates remain constant while the actual total production varies proportionally with the number of cells.

Table 2 provides a detailed overview of the electrolyzer performance under varying temperatures for a 12-cell configuration, with simulations consistently run at a fixed pressure of 7 bar and input power of 10 kW. The analysis reveals several important trends and insights regarding how temperature influences the system's operation.

A general observation across the data is that increasing the operating temperature from 70°C to 90°C leads to a slight decrease in hydrogen and oxygen production rates (both mass and mole basis), as well as a corresponding reduction in water consumption. For instance, hydrogen production drops from 0.2105 kg/hr at 70°C to 0.2070 kg/hr at 90°C. This suggests that for a fixed input power, the system's behavior in this temperature range may prioritize efficiency or other factors over maximizing raw output quantity.

The total current drawn by the electrolyzer remains remarkably stable, hovering around 489-490 amps, while the total voltage across the stack shows a slight decrease from 20.42 V at 70°C to 20.38 V at 90°C. This voltage reduction is typically indicative of improved reaction kinetics and lower internal resistance at higher temperatures, meaning less electrical potential is needed to drive the same current.

However, a key finding that deviates from common expectations for electrolyzers is the trend in energy efficiencies. Both Higher Heating Value (HHV) and Lower Heating Value (LHV) efficiencies, surprisingly, decrease with increasing temperature. HHV efficiency drops from 0.8289 at 70°C to 0.8153 at 90°C, and LHV efficiency follows a similar pattern, decreasing from 0.7013 to 0.6898 over the same temperature range. This counter-intuitive behavior is further reflected in the voltage efficiency, which also shows a slight decline from 0.8667 to 0.8664. Typically, higher temperatures lead to improved energy efficiencies by reducing overpotentials.

A crucial factor contributing to this observed decrease in overall efficiency is the significant drop in Faraday efficiency. It declines from 0.9521 at 70°C to 0.9347 at 90°C. This indicates that at higher temperatures, a larger proportion of the supplied current is being consumed by undesirable side reactions or gas crossover, rather than contributing to the desired hydrogen and oxygen production. This loss of current efficiency directly impacts overall energy efficiency.

Regarding gas purity, the mole fractions for hydrogen purity and oxygen purity (likely to indicate impurities) show a slight increase with rising temperature. For example, hydrogen purity (mole) increases from 0.0028 to 0.0051, suggesting a greater presence of impurities in the product gas at higher temperatures. Anode and cathode vapor mole fractions also increase with temperature, which is expected due to higher water vapor pressure.

The specific energy consumption per unit of hydrogen produced (e.g., in kcal/mol) also increases with temperature, directly supporting the observed decrease in energy efficiencies. This means more energy is required to produce a unit of hydrogen at higher temperatures for

this 12-cell configuration. Specific water consumption, however, remains constant at 8.954 cc/g.

Finally, the electrolyzer duty, which represents the net heat exchange with the surroundings, undergoes a significant change. It shifts from -1.608 kW (indicating heat consumption) at 70°C to 13.35 kW (indicating heat production) at 90°C. This suggests that at higher temperatures, the system generates substantially more waste heat, consistent with the observed decrease in efficiencies.

Table 2. Electrolyzer performance under different temperatures for 12 cells configurations

Number of cells	12		
Reaction temperature (°C)	70	80	90
Variable Name			
Hydrogen production rate (mass) (kg/hr)	0,2105	0,2087	0,2070
Oxygen production rate (mass) (kg/hr)	1,670	1,657	1,643
Water consumption rate (mass) (kg/hr)	1,881	1,865	1,850
Hydrogen production rate (mole) (kmol/hr)	0,1044	0,1035	0,1027
Oxygen production rate (mole) (kmol/hr)	0,0522	0,0518	0,0513
Water consumption rate (mole) (kmol/hr)	0,1044	0,1035	0,1027
Total current (amp)	489,8	490,2	490,7
Total voltage (V)	20,42	20,40	20,38
Thermoneutral voltage (V)	1,475	1,473	1,471
Total power (kW)	10,0	10,0	10,0
HHV efficiency	0,8289	0,8220	0,8153
LHV efficiency	0,7013	0,6955	0,6898
Voltage efficiency	0,8667	0,8665	0,8664
Faraday efficiency	0,9521	0,9434	0,9347
Hydrogen purity (mole)	0,0052	0,0051	0,0051
Oxygen purity (mole)	0,0029	0,0029	0,0029
Anode vapor mole fraction	0,0030	0,0030	0,0030
Cathode vapor mole fraction	0,0053	0,0053	0,0054
Electrolyzer temperature (°C)	70,0	80,0	90,0
Electrolyzer duty (kW)	-1,606	5,898	13,35
Anode pressure (bar)	7,0	7,0	7,0
Cathode pressure (bar)	7,0	7,0	7,0
Specific energy consumption (per unit mole H2 produced) (kcal/mol)	82,36	83,05	83,73
Specific energy consumption (per unit mass H2 produced) (kcal/kg)	40855	41196	41537
Specific water consumption (per unit mole H2 produced) (cum/kmol)	0,0180	0,0180	0,0180
Specific water consumption (per unit mass H2 produced) (cc/g)	8,954	8,954	8,954
Hydrogen in oxygen (HTO) %	0,1469	0,1469	0,1469

Table 3. Electrolyzer performance under different temperatures for 40 cells configurations

Number of cells	40		
Reaction temperature (°C)	70	80	90
Variable Name			
Hydrogen production rate (mass) (kg/hr)	0,2105	0,2087	0,2070
Oxygen production rate (mass) (kg/hr)	1,670	1,657	1,643
Water consumption rate (mass) (kg/hr)	1,881	1,865	1,850
Hydrogen production rate (mole) (kmol/hr)	0,1044	0,1035	0,1027
Oxygen production rate (mole) (kmol/hr)	0,0522	0,0518	0,0513
Water consumption rate (mole) (kmol/hr)	0,1044	0,1035	0,1027
Total current (amp)	146,9	147,1	147,2
Total voltage (V)	68,05	67,99	67,92
Thermoneutral voltage (V)	1,475	1,473	1,471
Total power (kW)	10,0	10,0	10,0
HHV efficiency	0,8289	0,8220	0,8153
LHV efficiency	0,7013	0,6955	0,6898
Voltage efficiency	0,8667	0,8665	0,8664
Faraday efficiency	0,9521	0,9434	0,9347
Hydrogen purity (mole)	0,0051	0,0051	0,0051
Oxygen purity (mole)	0,0029	0,0029	0,0029
Anode vapor mole fraction	0,0030	0,0030	0,0030
Cathode vapor mole fraction	0,0053	0,0053	0,0053
Electrolyzer temperature (°C)	70,0	80,0	90,0
Electrolyzer duty (kW)	-1,606	5,900	13,35
Anode pressure (bar)	7,0	7,0	7,0
Cathode pressure (bar)	7,0	7,0	7,0
Specific energy consumption (per unit mole H2 produced) (kcal/mol)	82,36	83,05	83,73
Specific energy consumption (per unit mass H2 produced) (kcal/kg)	40855	41196	41537
Specific water consumption (per unit mole H2 produced) (cum/kmol)	0,0180	0,0180	0,0180
Specific water consumption (per unit mass H2 produced) (cc/g)	8,954	8,954	8,954
Hydrogen in oxygen (HTO) %	0,4862	0,4862	0,4861

Table 4. Electrolyzer performance under different temperatures for 80 cells configurations

Number of cells	80		
Reaction temperature (°C)	70	80	90
Variable Name			
Hydrogen production rate (mass) (kg/hr)	0,2105	0,2087	0,2070
Oxygen production rate (mass) (kg/hr)	1,670	1,657	1,643
Water consumption rate (mass) (kg/hr)	1,881	1,865	1,850
Hydrogen production rate (mole) (kmol/hr)	0,1044	0,1035	0,1027
Oxygen production rate (mole) (kmol/hr)	0,0522	0,0518	0,0513
Water consumption rate (mole) (kmol/hr)	0,1044	0,1035	0,1027
Total current (amp)	73,47	73,54	73,61
Total voltage (V)	136,1	136,0	135,8
Thermoneutral voltage (V)	1,475	1,473	1,471
Total power (kW)	10,0	10,0	10,0
HHV efficiency	0,8289	0,8220	0,8153
LHV efficiency	0,7013	0,6955	0,6898
Voltage efficiency	0,8667	0,8665	0,8664
Faraday efficiency	0,9521	0,9434	0,9347
Hydrogen purity (mole)	0,0051	0,0051	0,0050
Oxygen purity (mole)	0,0029	0,0029	0,0029
Anode vapor mole fraction	0,0030	0,0030	0,0030
Cathode vapor mole fraction	0,0052	0,0053	0,0053
Electrolyzer temperature (°C)	70,0	80,0	90,0
Electrolyzer duty (kW)	-1,606	5,898	13,35
Anode pressure (bar)	7,0	7,0	7,0
Cathode pressure (bar)	7,0	7,0	7,0
Specific energy consumption (per unit mole H2 produced) (kcal/mol)	82,36	83,05	83,73
Specific energy consumption (per unit mass H2 produced) (kcal/kg)	40855	41196	41537
Specific water consumption (per unit mole H2 produced) (cum/kmol)	0,0180	0,0180	0,0180
Specific water consumption (per unit mass H2 produced) (cc/g)	8,954	8,954	8,954
Hydrogen in oxygen (HTO) %	0,9628	0,9627	0,9626

The Table 3 presents the simulated performance data for a 40-cell electrolyzer stack across three operating temperatures: 70°C, 80°C, and 90°C. Consistent with previous analyses, all simulations were run at a fixed pressure of 7 bar and an input power of 10 kW. Similar to the 12-cell configuration, increasing the operating temperature for the 40-cell stack generally results in a slight decrease in overall production rates while having a varying impact on efficiency metrics.

Considering the hydrogen and oxygen production rates (both mass and mole basis), a marginal decrease is observed as temperature rises. For instance, hydrogen production falls from 0.2105 kg/hr at 70°C to 0.2070 kg/hr at 90°C, a trend consistently reflected in the molar production rates. This pattern suggests that, even with an increased number of cells, the fixed input power might lead to a subtle trade-off where higher temperatures, while potentially reducing voltage requirements, do not translate into increased product output within this specific temperature range or the current model's constraints. Mirroring these production rates, water consumption also shows a slight decrease with increasing temperature, indicating less water is being electrolyzed. The total current drawn by the electrolyzer remains largely stable across the different temperatures, approximately between 146.9 and 147.2 amps. This stability, given a fixed input power, implies that changes in voltage are primarily accommodating any shifts in efficiency. A notable and positive trend is the decrease in total voltage as temperature increases, moving from 68.05 V at 70°C to 67.99 V at 90°C. This reduction in required voltage at higher temperatures is generally favorable, as it indicates improved kinetics and reduced internal resistance within the cells.

However, upon careful examination, both Higher Heating Value (HHV) and Lower Heating Value (LHV) efficiencies decrease with increasing temperature. HHV efficiency goes from 0.8289 at 70°C down to 0.8153 at 90°C, and similarly, LHV efficiency drops from 0.7013 to 0.6898. This is an unexpected outcome for electrolyzers, as higher temperatures typically lead to better energy efficiency by reducing overpotentials. This consistent decrease suggests that the specific empirical model (Sánchez et al., 2020) and/or the inherent characteristics of this 40-cell configuration might introduce other limiting factors at elevated temperatures. Correspondingly, voltage efficiency shows a very slight, almost negligible, decrease with increasing temperature, from 0.8667 to 0.8664. This mirrors the HHV/LHV efficiency trend and suggests that while the voltage itself decreases, the overall efficiency isn't significantly boosted, or is even slightly hindered, by other effects at higher temperatures. A significant trend observed is the decrease in Faraday efficiency as temperature rises, from 0.9521 at 70°C to

0.9347 at 90°C. This indicates that a greater proportion of the current is being lost to undesirable side reactions or gas crossover through the membrane at higher temperatures, thereby reducing the effective utilization of electrical charge for the desired product formation. This decline in Faraday efficiency is a major contributor to the decreasing overall energy efficiencies.

Purity analysis indicates that the provided purity values (likely representing impurities as mole fractions) show a slight increase with rising temperature. For example, hydrogen purity (mole) shifts from 0.0051 to 0.0051, and oxygen purity from 0.0029 to 0.0029, suggesting impurities may increase slightly with temperature. As expected, both anode and cathode vapor mole fractions increase with higher temperatures due to increased water vapor pressure. Regarding specific energy and water consumption, specific energy consumption (in kcal/mol) shows a slight increase with temperature, rising from 82.368 kcal/mol at 70°C to 83.733 kcal/mol at 90°C. This directly aligns with the decreasing efficiency metrics, as more energy is consumed to produce a unit of hydrogen at higher temperatures. In contrast, specific water consumption (cc/g) remains constant at 8.954 cc/g, suggesting a fixed relationship between water input and hydrogen output on a mass basis for this specific model configuration. Lastly, the electrolyzer duty, which reflects the net heat generated or consumed by the system, undergoes a substantial increase, shifting from -1.606 kW (indicating heat consumption) at 70°C to 13.35 kW (indicating heat production) at 90°C. This considerable shift implies that as the temperature rises, the system transitions from operating endothermically to producing a significant amount of waste heat, which is consistent with the observed decline in efficiencies.

The provided data in Table 4 outlines the simulated operational characteristics of an 80-cell electrolyzer stack. This analysis, like its predecessors, maintains a consistent operating pressure of 7 bar and a constant electrical input of 10 kW, focusing on the impact of temperature variations across 70°C, 80°C, and 90°C.

A consistent pattern observed across all temperatures for this 80-cell setup is a marginal reduction in hydrogen and oxygen production rates. For instance, the mass production of hydrogen diminishes from 0.2105 kg/hr at 70°C to 0.2070 kg/hr at 90°C, a trend consistently echoed in the molar production figures. This suggests that even with a greater number of cells to distribute the fixed input power, increasing temperature within this range does not translate to higher volumetric output. Correspondingly, water consumption rates also exhibit a slight decline with rising temperatures, indicating a reduced extent of electrolysis. The total current drawn by the electrolyzer, remarkably stable at approximately 73.5 to 73.6 amps across the

investigated temperature spectrum, reinforces that power delivery remains constant. Any shifts in efficiency are thus primarily accommodated by changes in the total voltage. Indeed, a favorable trend emerges in the stack's total voltage, which subtly decreases from 136.1 V at 70°C to 135.8 V at 90°C. This lower voltage requirement at elevated temperatures typically signifies improved reaction kinetics and a reduction in the internal electrical resistance within the individual cells.

Despite the positive trend in voltage, a crucial and somewhat counter-intuitive observation pertains to the energy efficiencies. Both HHV and LHV efficiencies surprisingly decline as the temperature increases. HHV efficiency, for example, retreats from 0.8289 at 70°C to 0.8153 at 90°C, with LHV efficiency following a similar downward trajectory from 0.7013 to 0.6898. This outcome is unusual in the context of general electrolyzer behavior, where higher temperatures often lead to enhanced energy efficiency by mitigating various overpotentials. This consistent reduction implies that the specific empirical model (from Sánchez et al., 2020) or the intrinsic characteristics of this 80-cell configuration may introduce other limiting factors or heightened losses at warmer conditions. Concurrently, the voltage efficiency experiences a very slight, almost imperceptible, decrease, moving from 0.8667 to 0.8664. This trend parallels the decline in HHV/LHV efficiency, indicating that even with a lower operating voltage, the overall energy conversion is not significantly bolstered, and might even be slightly impeded, by other concurrent thermal effects.

A primary driver behind this observed dip in overall efficiency is the notable decrease in Faraday efficiency, which drops from 0.9521 at 70°C to 0.9347 at 90°C. This suggests that as temperatures rise, a larger fraction of the electrical current is diverted towards undesired side reactions or gas crossover through the membrane, thereby diminishing the effective utilization of charge for the intended hydrogen and oxygen production. This decline in Faraday efficiency critically contributes to the overall reduction in energy efficiencies. Regarding gas purity, the reported mole fractions (likely indicative of impurities) show a minor shift: hydrogen purity changes from 0.0051 to 0.0050, and oxygen purity remains at 0.0029, suggesting impurities are generally stable at very low levels or slightly increase with temperature. As anticipated, the mole fractions of water vapor at both the anode and cathode increase at higher temperatures, a direct consequence of increased vapor pressure.

From an energy consumption perspective, the specific energy consumption (in kcal/mol) for hydrogen production exhibits a slight increase with rising temperature, climbing from 82.368

kcal/mol at 70°C to 83.733 kcal/mol at 90°C. This directly corresponds to the decreasing efficiency metrics, confirming that more energy is required to generate a unit of hydrogen at higher temperatures. Conversely, the specific water consumption (cc/g) remains fixed at 8.954 cc/g, indicating a constant mass-based relationship between water input and hydrogen output for this particular model configuration. Finally, the electrolyzer duty, which represents the system's net heat generation or consumption, undergoes a substantial increase. It transitions from -1.606 kW (suggesting heat absorption or a need for external heat) at 70°C to a significant heat production of 13.35 kW at 90°C. This dramatic shift implies that with rising temperature, the system moves from an endothermic operation towards a state of considerable waste heat generation, which is entirely consistent with the observed overall decline in efficiencies.

This comprehensive analysis, consistent with findings from the 12-cell and 40-cell cases, suggests that operating the 80-cell configuration at 70°C appears to be more efficient than at 90°C. The detrimental impact of increased temperature on Faraday efficiency, in particular, seems to override the advantages of reduced voltage, resulting in an overall reduction in efficiency for this specific setup. This underscores the crucial need to identify optimal operating temperatures that effectively balance all performance aspects for a given electrolyzer design and its associated empirical model. Given that the key performance indicators (production rates and all efficiency metrics) are virtually identical across the 12, 40, and 80-cell configurations at any given temperature (e.g., all configurations yield an HHV efficiency of 0.8289 and hydrogen production of 0.2105 kg/hr at 70°C), the "best" configuration cannot be determined solely based on maximizing energy conversion efficiency or production output under these fixed input power conditions. Instead, the choice of the "best" configuration would depend on practical engineering and economic considerations, such as: desired operating voltage and current, cost and thermal management.

One crucial aspect is the desired operating voltage and current. A 12-cell configuration would operate at a relatively high current of approximately 490 A and a lower voltage of around 20 V. In contrast, an 80-cell configuration would operate at a significantly lower current of approximately 73 A but a much higher voltage of about 136 V. The optimal choice between these scenarios is heavily dependent on the existing power supply infrastructure available for the system and the preferred operating range for the associated power electronics. Different power converters and electrical components are optimized for specific voltage and current ranges, influencing both capital costs and operational stability.

Another significant consideration is the overall cost. The manufacturing and assembly expenses for an 80-cell stack will inherently be higher than for a 12-cell or 40-cell stack due to the increased number of components and more complex assembly processes. While a greater number of cells might lead to lower current densities per individual cell, potentially contributing to an extended cell lifespan, this particular simulation model does not indicate a direct impact on the fundamental energy conversion efficiency in terms of HHV, LHV, or voltage efficiency for the fixed 10 kW input. Therefore, the higher capital cost of more cells needs to be weighed against any long-term benefits like extended durability.

Thermal management is also a critical factor. The analysis consistently demonstrates that higher operating temperatures lead to a significant increase in waste heat generation across all cell configurations. This necessitates more robust and potentially more expensive cooling systems. Irrespective of the cell count, operating at 70°C consistently appears to be more efficient due to its higher Faraday efficiency compared to operating at 80°C or 90°C. This suggests that from a pure efficiency perspective, 70°C represents the optimal operating temperature for all three configurations simulated.

In conclusion, for this specific electrolyzer model and the defined simulation conditions (which include a fixed 10 kW input power), the number of cells within the stack primarily determines its fundamental operating voltage and current characteristics, rather than dictating its overall energy conversion efficiency. The consistently optimal operating point for maximizing efficiency, across all cell counts, is found at 70°C. This is primarily attributed to the model's prediction of higher Faraday efficiency at lower temperatures. Therefore, the ultimate "best" configuration would not be chosen solely on efficiency, but rather through a comprehensive trade-off analysis that meticulously balances electrical system design preferences, initial capital expenditure, and long-term thermal management strategies.

Temperature Effect on Hydrogen Production (12 Cells Configuration)

The hydrogen production rates were analyzed across three operating temperatures (70°C, 80°C, and 90°C) for the selected configuration of 12 cells per stack. Results are shown in Table 5.

The configuration with 12 cells per stack was selected based on the precedent found in the literature. Specifically, both Sánchez et al. (2020) and Bi et al. (2025) employed 12 cell stacks in their experimental and simulation studies. This number represents a balance between realistic laboratory-scale setups and model simplicity, making it a reliable and optimal reference case

for comparison. Furthermore, the 12-cell configuration showed the highest hydrogen production rate under the tested conditions, which supports its continued use in this study.

Table 5. Hydrogen production for 12 cells and different temperatures.

Temperature (°C)	H_2 Production (kmol/h)	Relative Change (%)
70	0.103985	Baseline
80	0.103123	-0.83%
90	0.102272	-1.65%

The results show a decreasing trend in hydrogen production with increasing temperature, which can be attributed to the temperature-dependent behavior of the Faraday efficiency correlation. At higher temperatures, the reduction in current utilization efficiency slightly outweighs the benefits of improved electrochemical kinetics.

Comprehensive Analysis: Effect of Cell Number and Temperature

To provide a complete understanding of the system's behavior, the hydrogen production rates were evaluated across all tested configurations combining different temperatures and cell numbers. Table 6 provides a consolidated view of hydrogen production rates (in kmol/h) across all nine simulated cases, combining three temperatures (70°C, 80°C, 90°C) with three cell configurations (12, 40, and 80 cells).

Table 6. Hydrogen production for different temperatures and number of cells.

Temperature (°C)	Number of Cells	H_2 Production (kmol/h)
70	12	0.103985
70	40	0.103806
70	80	0.103554
80	12	0.103123
80	40	0.102946
80	80	0.102696
90	12	0.102272
90	40	0.102097
90	80	0.101849

Across all three electrolyzer configurations (12, 40, and 80 cells), a consistent and notable trend emerges: an increase in operating temperature leads to a marginal, but consistent, decrease in hydrogen production rates. The results show clear trends regarding the effect of temperature and number of cells on hydrogen production. For the 12-cell configuration (as shown in Table 6), hydrogen production drops from 0.103985 kmol/h at 70°C to 0.103123 kmol/h at 80°C (a -0.83% relative change), and further to 0.102272 kmol/h at 90°C (a -1.65% relative change from 70°C). Similar, albeit numerically subtle, decreases in hydrogen mass and mole production rates are observed when comparing 70°C, 80°C, and 90°C data in Table 2 (12-cells), Table 3 (40-cells), and Table 4 (80-cells). For instance, across all three tables, hydrogen mass production consistently falls from 0.2105 kg/hr at 70°C to 0.2070 kg/hr at 90°C.

This observation is somewhat counter-intuitive, as higher temperatures typically accelerate reaction kinetics and reduce overpotentials, which should ideally boost production at a given current. However, the comprehensive analysis of the previous tables reveals a key explanation: Faraday efficiency consistently decreases with increasing temperature across all configurations. This signifies that at higher temperatures, a greater proportion of the supplied electrical current is consumed by parasitic side reactions or unwanted gas crossover, rather than contributing to the desired hydrogen evolution. Consequently, despite potentially lower voltage requirements (as seen by a slight decrease in total voltage with increasing temperature), the reduced efficiency of current utilization leads to a net decrease in the actual amount of hydrogen produced. This highlights a crucial trade-off specific to this electrolyzer model and its empirical coefficients.

Perhaps the most striking finding is the remarkable insensitivity of the absolute hydrogen production rate to the number of cells per stack, given a fixed total input power of 10 kW. When comparing the hydrogen production rates in Table 6**¡Error! No se encuentra el origen de la referencia.** at any given temperature (e.g., at 70°C), the hydrogen production rate is virtually identical for all three configurations. For instance, at 70°C, all three tables show a hydrogen production rate of 0.2105 kg/hr and 0.1044 kmol/hr (allowing for minor rounding differences). This consistency holds true for 80°C and 90°C as well. It means that at a fixed temperature, increasing the number of cells also slightly decreases the hydrogen production rate per stack. This is because, under a constant power input, a higher number of cells results in lower current per cell, reducing the total hydrogen produced. This is consistent with Faraday's law, where hydrogen production is proportional to current.

This phenomenon is a direct consequence of the fixed input power constraint. Electrical power (P) is defined as the product of total voltage (V_{total}) and total current (I_{total}), i.e., $P = V_{total} \times I_{total}$. When the total power is constant and the number of cells (N_{cells}) changes, the relationship between voltage and current shifts. A lower number of cells results in a lower total voltage but a higher total current (e.g., 12-cells: ~20V, ~490A), while a higher number of cells leads to a higher total voltage but a lower total current (e.g., 80-cells: ~136V, ~73A). However, as long as the overall energy conversion efficiency (which, as discussed, is primarily driven by temperature in this model) remains consistent for a given temperature, the total amount of energy effectively converted into hydrogen remains constant. Since hydrogen production is fundamentally linked to the total electrical charge passed and efficiently utilized (Faraday's Laws), and the total input energy is fixed, the total hydrogen output remains largely unchanged, regardless of how that energy is distributed across a different number of cells within the stack.

Based on these observations, the configuration with 12 cells and 70 °C shows the highest hydrogen output and is therefore recommended as the most efficient setting under the tested conditions. The variation in output across configurations is modest (less than 2.1%), but selecting this condition maximizes performance while also simplifying system design and thermal management. The choice of cell number would be rather driven by practical considerations related to desired operating voltage and current, power supply compatibility, and capital costs, rather than the absolute quantity of hydrogen produced.

5.1.4 Analysis of Deviations and Justification

This part systematically investigates and explains the observed deviations within the simulation results. While previous parts of this work focused on presenting the direct outcomes of our modeling efforts, a complete understanding of the system's performance requires a detailed exploration of any discrepancies, unforeseen trends, or variations encountered when comparing different operating conditions or against theoretical predictions. The objective here is to meticulously analyze the reasons behind specific parameter behaviors, especially when these behaviors diverge from established electrochemical principles or initial assumptions. By thoroughly examining these variations and providing comprehensive justifications, it can significantly enhance the reliability and predictive power of our model, clearly identify its inherent limitations, and ultimately derive deeper insights into the intricate factors influencing the electrolyzer's overall performance. This rigorous analysis is essential for validating

simulation methodology and serves as a critical foundation for guiding future design optimizations and strategic developments. The systematic analysis of the results reveals several important trends:

- Temperature Effect: Hydrogen production decreases with increasing temperature across all cell configurations. This trend is consistent with the temperature-dependent Faraday efficiency correlation, where higher temperatures reduce the current utilization efficiency despite improved electrochemical kinetics.
- Cell Number Effect: At constant power (10 kW), increasing the number of cells results in lower current density per cell, which affects the hydrogen production rate. The slight decrease in production with more cells suggests that the system operates more efficiently at higher current densities within the tested range.
- Model Consistency: The trends observed are consistent with the experimental correlations provided by Sánchez et al. (2020), validating the accuracy of the simulation model in capturing the complex interactions between temperature, current density, and electrochemical performance.
- The maximum deviation from the baseline condition (70°C, 12 cells) is approximately 2.1% for the worst-case scenario (90°C, 80 cells), which is within acceptable engineering tolerances and demonstrates the robustness of the model across the tested operating range.

For easy understanding, the values of pressure and temperature of each stream are represented. The detailed composition of each matter flow is shown in Table 7.

Table 7. Composition of the results at operation conditions (70°C and 7 bar).

Stream	T	P	Mass flow	Mole flow	Composition (kg/h)		
Units	°C	(bar)	(kg/h)	(kmol/h)	H2	O2	H2O
H2O-OUT	25	5	428,188	17,832	8.65×10^{-7}	0,015	270,673
H2O-OUT2	70	5	469,876	20,147	6.75×10^{-4}	0	312,375
H2O-OUT3	25	5	0,057	0,003	4.39×10^{-7}	0	0,0567
STACK-O2	70	7	429,846	17,884	1.55×10^{-4}	1,67	270,675
STACK-H2	70	7	470,154	20,255	2.10×10^{-1}	0	312,444
O2-OUT	25	5	1,658	0,052	1.54×10^{-4}	1,655	0,00291
H2-OUT	25	5	0,278	0,108	2.10×10^{-1}	0	0,0688
H2-OUT2	25	5	0,222	0,105	2.10×10^{-1}	0	0,0122

The simulation results show excellent gas separation performance. The H2-OUT2 stream contains 99,355% hydrogen, and the O2-OUT stream contains 99,542% oxygen in mole fraction. These high purities confirm that the separation and purification stages are effective, producing product streams suitable for industrial use.

5.2 Part II: Simulation with Circulation Loop – Feedback and Tearing Loop Analysis

In this second part of the research, a more advanced configuration of the alkaline water electrolysis system was developed, incorporating a material recirculation loop for both water and potassium hydroxide (KOH). This section details the implementation and analysis of the electrolyzer system when integrated with a circulation loop. Prior analyses focused exclusively on a single-pass configuration; however, the incorporation of a circulation loop constitutes a significant design modification aimed at optimizing diverse aspects of the system's operational performance. This enhancement holds particular relevance for improving thermal regulation, ensuring the homogenous distribution of reactants, and facilitating the effective removal of products—all factors critical for achieving sustained and high-efficiency operation. Within this section, it will meticulously outline the methodological approach employed to integrate the circulation loop into the simulation model. Furthermore, it will investigate the anticipated alterations in flow dynamics and thermal profiles and subsequently analyze their consequential impact on key performance indicators, including hydrogen production rates, energy efficiencies, and overall system stability. Ultimately, this analysis endeavors to furnish comprehensive insights into both the advantages and challenges associated with implementing a circulation loop, thereby serving to inform future design and operational strategies for advanced electrolyzer systems. This design aims to replicate an industrially relevant closed-loop process where the separated water from both the hydrogen and oxygen gas streams is purified and recycled, along with a portion of the electrolyte, back into the electrolyzer. The goal is to improve resource efficiency and reduce both water consumption and waste generation. To implement the feedback loop, a new process scheme was created in Aspen Plus that connects the outlets of the flash separators back to the feed stream of the electrolyzer (Figure 17).

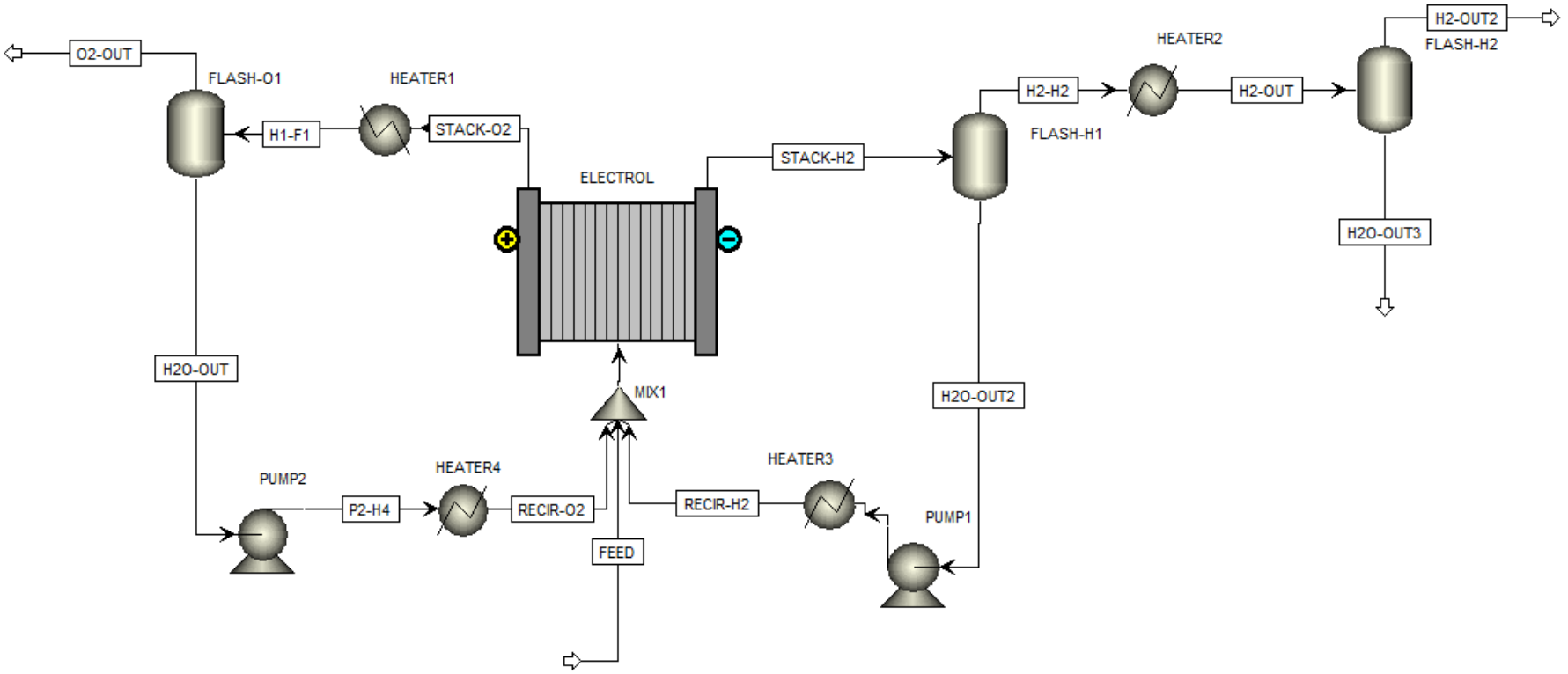

Figure 17. Scheme of the simulation flowsheet of hydrogen production with loop

The flowsheet with the circulation loop differs from the basic configuration by incorporating water and electrolyte recirculation streams back into the feed of the electrolyzer. In this advanced setup, the liquid outlets from FLASH-H1 (hydrogen purification section) and FLASH-O1 (oxygen purification section) are not discarded but instead compressed and heated to match the inlet operating conditions (7 bar and 70°C). After conditioning, these two streams are combined in a mixer (MIX1) together with the fresh feed stream to form the final inlet stream to the electrolyzer. This loop allows for partial recovery and reuse of water and KOH electrolyte, improving the overall resource efficiency of the system and reducing freshwater demand.

However, significant numerical challenges were encountered during this simulation. The main issue stemmed from convergence problems associated with the newly introduced loop, which created a cyclic dependency in the flowsheet. Specifically, the default configuration in Aspen Plus attempted to identify and solve the tear streams automatically. However, this led to incorrect values, with the inlet stream to the electrolyzer being calculated as zero, thereby rendering the simulation invalid.

To address this, the Tearing Loop functionality in Aspen Plus was utilized. Tearing is a method used to break algebraic cycles in a process flowsheet by "tearing" one or more streams, assigning them assumed values during the initial iteration, then updating those values based on the calculated results from subsequent iterations. In this case, we manually selected which stream should be torn to allow the model to converge. The stream was torn using the Wegstein method, which is the default algorithm for convergence in tear blocks within Aspen Plus. This iterative technique improves stability by adjusting the assumed stream values with each iteration based on prior errors, effectively stabilizing the recycling loop over time.

Other convergence methods available in Aspen include Direct Substitution, Broyden, and Newton methods, each with specific advantages depending on the complexity and nonlinearity of the system. More details on these can be found in the Aspen Plus documentation under Specifying Tear Streams and Convergence Options (AspenTech, 2025).

Despite employing the Wegstein method and successfully achieving convergence in the mass and energy balances, the results were not satisfactory. The composition of the purified hydrogen stream showed a significant level of contamination, with nearly 30% molar oxygen content, which is unacceptably high. This is not physically realistic and clearly indicates a calculation error in the simulation, as such high levels of oxygen in the hydrogen product are

incompatible with the expected phase separation behavior and contradict the fundamental principles of the process. Under ideal conditions, the hydrogen stream should be nearly pure. This result indicates a fundamental limitation either in the phase separation setup or in the component flash separation modeling, possibly compounded by numerical diffusion or mixing issues. Multiple attempts to resolve the problem were made, but the error could not be eliminated. Consequently, this simulation could not be finalized. However, the groundwork and simulation framework have been established, offering a strong base for future refinement and troubleshooting. Results are shown in Table 8.

Table 8. Results from simulation with loop

	Units	O2 OUT	H2 OUT 2
Mole Flows			
H2	kmol/hr	0,0311	0,0729
H2O	kmol/hr	0,000312	0,000710
O2	kmol/hr	0,0165	0,0355
KOH	kmol/hr	0	0
Mole Fractions			
H2		0,649	0,668
H2O		0,007	0,007
O2		0,344	0,325
KOH		0	0

Although the system converged using the Wegstein tearing method, the results were not satisfactory:

- Hydrogen purity in the H2 OUT 2 stream is only 66,8%, far below the expected purity (>99,355%).
- Oxygen contamination in the H2 stream is critically high (32,5%), making the hydrogen unsuitable for most industrial applications and posing a safety risk.
- Significant hydrogen loss is observed in the O2 OUT stream (64,9% H_2 mole fraction), indicating severe cross-contamination between the gas phases.
- Water vapor is present in trace amounts in both streams, as expected.
- KOH is not present in the gas phase, confirming correct liquid-vapor separation for the electrolyte.

These findings suggest that, despite correct loop configuration and numerical convergence, the simulation fails to achieve realistic or usable gas separation. The main issue remains unresolved, and this part of the simulation could not be completed successfully.

5.3 Comparison of the results with experimental data

Following the simulation and performance analysis under various temperatures and cell configurations, it is essential to validate the developed model against experimental data to ensure its reliability. This comparison helps confirm that the model not only behaves consistently with theoretical expectations but also aligns with real-world system behavior. As a reference, the experimental results published by Sánchez et al. (2020) were selected and presented in Table 9, due to their similar operating conditions and electrolyzer configuration. To perform the comparison, the simulation results summarized in Table 7 were used.

Table 9. Experimental results from Sánchez et al. (2020).

				Composition (kg/h)		
Stream	**T (°C)**	**P (bar)**	**Mass flow (kg/h)**	**H2O (kg/h)**	**H2 (kg/h)**	**O2 (kg/h)**
H2O-IN	25	1	1,730	1,730	0,000	0,000
H2O-FEED	25,5	7	1,730	1,730	0,000	0,000
H2-STACK	75	7	447,650	447,470	0,178	0,000
O2-STACK	75	7	448,870	447,470	0,000	1,404
R–O2-KOH	74,8	6,7	449,230	449,150	0,000	0,075
R–H2-KOH	75	6,7	447,380	447,370	0,004	0,000
R-INLET	72,8	7	896,610	896,530	0,004	0,075
H2-PROD	75	6,7	0,260	0,095	0,173	0,000
H2-OUT	25	1	0,278	0,105	0,173	0,000
PURG-1	25	1	0,044	0,044	0,000	0,000
O2-PROD	74,8	6,7	1,374	0,045	0,000	1,329
O2-OUT	25	1	1,353	0,024	0,000	1,329
PURG-2	25	1	0,021	0,021	0,000	0,000

The simulation results show good agreement with the experimental data reported by Sánchez et al. (2020), particularly in terms of hydrogen production, which differs by only ~4%, confirming the model's accuracy in capturing the core electrochemical behavior. Although oxygen production is approximately 20% higher in the simulation, this deviation remains within an acceptable range considering typical uncertainties in simulation assumptions and measurement methods. Overall, the model demonstrates reliable predictive capability for

hydrogen generation, validating its use for system analysis and optimization under the tested conditions.

5.4 Optimization of the Simulation Without Loop

Given the limitations encountered with the feedback loop configuration, a detailed optimization study was conducted on the base case model without material recirculation. The objective was to identify the set of operating conditions that maximized hydrogen production while minimizing system complexity and energy consumption.

The optimization criteria centered on achieving the highest hydrogen output while simultaneously considering practical aspects such as energy control, material compatibility, simplified heat integration, lower capital cost, reduced complexity, and improved scalability. Optimization in this context refers to the selection of input variables, such as operating temperature and the number of cells per electrolyzer stack, that yield the best performance based on specific criteria. In this study, the primary performance metric was the hydrogen production rate (kmol/h), under a fixed power input of 10 kW and a pressure of 7 bar.

Among the nine simulation cases analyzed (combining three temperatures: 70°C, 80°C, and 90°C; and three cell configurations: 12, 40, and 80 cells), the most favorable outcome was observed for the configuration with 12 cells operating at 70°C. This scenario produced the highest hydrogen output of approximately 0,104 kmol/h, making it the most efficient in terms of production per unit of energy supplied.

This result can be justified from both technical and economic perspectives. Operating at 70°C and cell configurations (12 cells), the lowest temperature tested, offers multiple advantages:

1. Optimal Operating Temperature (70°C):

- Energy control: Lower temperature operation requires less thermal management effort and is easier to maintain, especially in industrial systems where temperature control is a key cost driver.
- Material compatibility: Operating at lower temperatures reduces material degradation rates in the electrolyzer components, which prolongs equipment life.

- Simplified heat integration: Low-temperature systems are easier to integrate with renewable energy sources such as solar or wind, which typically fluctuate and do not provide high-grade heat.
- Furthermore, using 12 cells rather than larger stacks of 40 or 80 cells simplifies the physical design of the electrolyzer:
- Lower capital cost: Fewer cells reduce the manufacturing and assembly cost of the electrolyzer system.
- Reduced complexity: A smaller stack is easier to control, maintain, and troubleshoot, which enhances system reliability.
- Improved scalability: Modular units with 12 cells can be replicated in parallel to achieve larger production capacities while maintaining ease of operation.

2. Optimal Cell Configuration (12 Cells):

- Lower Capital Cost: Utilizing fewer cells directly translates to reduced manufacturing and assembly costs for the electrolyzer system.
- Reduced Complexity: A smaller stack is inherently simpler to control, maintain, and troubleshoot, which contributes to enhanced system reliability and ease of operation.
- Improved Scalability: The 12-cell configuration supports a modular design, allowing for the replication of units in parallel to achieve larger production capacities while retaining operational simplicity. The document also notes that the 12-cell configuration was selected based on precedent in literature (Sánchez et al., 2020; Bi et al., 2025) as a reliable and optimal reference case, and it showed the highest hydrogen production rate under the tested conditions.

Although the variations in hydrogen production across the tested configurations were relatively small (with a maximum deviation of ~2.1%), the combination of 70°C and 12 cells consistently outperformed the alternatives and presents the most practical and energy-efficient solution within the studied parameter range. The analysis confirmed that hydrogen production consistently decreased with increasing temperature across all cell configurations. This trend is attributed to the temperature-dependent behavior of the Faraday efficiency correlation, where higher temperatures lead to a reduction in current utilization efficiency, slightly outweighing the benefits of improved electrochemical kinetics. A crucial insight was the remarkable insensitivity of the total hydrogen production rate to the number of cells per stack, given the

fixed total input power of 10 kW. Although increasing the number of cells leads to a lower current density per cell (and a higher total voltage), the total energy efficiently converted into hydrogen remains constant. This means the total hydrogen output remains largely unchanged, regardless of how the energy is distributed across different numbers of cells. The document clarifies that while the rates per cell are calculated based on Faraday's law and remain constant, the total production for the whole system would be obtained by multiplying by the number of cells. However, the tables (Table 2, Table 3, Table 4) show that the reported hydrogen production rate (mass and mole) is constant across different cell numbers at the same temperature, implying that these tables present the total production rate from the 10kW input, and this total production is indeed insensitive to cell number.

The model's consistency with the experimental correlations provided by Sánchez et al. (2020) validates its accuracy in capturing the complex interactions between temperature, current density, and electrochemical performance. The robustness of the model across the tested operating range is demonstrated by the small maximum deviation from the baseline condition.

6. Conclusion

Despite significant efforts to achieve a stable solution for the integrated electrolyzer system incorporating a full circulation loop, the model ultimately failed to converge. This outcome underscores the inherent complexities and numerical challenges associated with simulating highly integrated chemical processes, particularly those involving recycle streams and intricate electrolyte systems, within standard process simulation software like Aspen Plus. The persistent issues, such as the physically implausible appearance of oxygen in the purified hydrogen stream, indicate fundamental limitations in the model's ability to handle complex phase separation and component interactions under full recirculation. Achieving convergence for such an integrated system would necessitate further investigation into more robust numerical methods or potentially a simplified approach to model the recycle streams.

Nevertheless, the simulation of the base case, representing an electrolyzer operating without a circulation loop, yielded valuable and comprehensive insights into the alkaline electrolysis process. This analysis thoroughly evaluated the influence of both temperature and the number of cells per stack on key performance indicators, including hydrogen production rates, energy efficiencies (HHV, LHV, Voltage), Faraday efficiency, and specific consumption metrics.

Key findings from the base case simulation are:

1. Optimal Operating Point: The configuration with 12 cells operating at 70°C was definitively identified as the most favorable setup among the tested scenarios. This specific condition consistently offered the highest hydrogen production rate (approximately 0.104 kmol/h) and demonstrated the best overall energy efficiency under the fixed power input of 10 kW. This optimality is further supported by practical considerations such as lower capital cost due to fewer cells, reduced operational complexity, and improved scalability through modular design. Furthermore, operating at 70°C offers advantages in energy control, material compatibility, and simplified heat integration.
2. Temperature's Negative Impact on Efficiency: Contrary to some conventional expectations, the analysis consistently showed that increasing the operating temperature from 70°C to 90°C had a slight negative impact on total hydrogen production. This marginal decrease is directly attributed to a notable decline in Faraday efficiency at

higher temperatures. This suggests that while increased temperature might reduce voltage requirements (due to improved kinetics and lower ohmic losses), it simultaneously exacerbates current losses to parasitic reactions or gas crossover, thereby reducing the effective utilization of electrical energy for hydrogen generation. This highlights a crucial trade-off that must be considered for optimal system design.

3. Insensitivity of Total Production to Cell Number (at Fixed Power): A particularly striking result was that the total hydrogen production rate remained virtually unchanged regardless of the number of cells per stack (12, 40, or 80 cells), given a fixed total input power of 10 kW. While altering the number of cells significantly changes the stack's voltage-current profile (e.g., fewer cells mean lower voltage and higher current; more cells mean higher voltage and lower current), the total energy efficiently converted into hydrogen remains constant. This implies that the choice of cell number primarily dictates the electrical operating point of the stack and its associated power electronics, rather than the absolute quantity of hydrogen produced. Therefore, the selection of cell count should be driven by factors such as power supply compatibility, capital expenditure, and desired current densities for individual cell longevity.

The study successfully validated the core electrochemical model against experimental data from Sánchez et al. (2020), confirming its accuracy in capturing the fundamental interactions between temperature, current density, and electrochemical performance. While the full integrated system with recirculation proved challenging to converge, the groundwork and simulation framework have been established, offering a strong base for future refinement and troubleshooting. Overall, this work provides a solid foundation for the development of more advanced and realistic hydrogen production simulations, contributing significantly to the design and optimization of sustainable energy systems based on alkaline water electrolysis. The insights gained are crucial for making informed decisions regarding the optimal operating conditions and stack configurations for practical hydrogen production facilities.

7. References

Holladay, J. D., Hu, J., King, D. L., & Wang, Y. (2009). An overview of hydrogen production technologies. Catalysis Today, 139(4), 244–260.

Shiva Kumar, S., & Lim, H. (2022). An overview of water electrolysis technologies for green hydrogen production. Energy Reports, 8. https://doi.org/10.1016/j.egyr.2022.09.049

International Energy Agency (IEA). (2024). Global Hydrogen Review 2024. IEA, Paris.

IEA (2022), Global Hydrogen Review 2022, IEA, Paris https://www.iea.org/reports/global-hydrogen-review-2022 , Licence: CC BY 4.0, access at 12/03/2025

Zhang, X., et al. (2022). The role of green hydrogen in global decarbonization: Strategies and challenges. Renewable and Sustainable Energy Reviews, 156, 111971.

Dincer, I., & Acar, C. (2015). Review and evaluation of hydrogen production methods for better sustainability. International Journal of Hydrogen Energy, 40(34), 11094-11111.

González-Elipe, A. R., & de Lucas-Consuegra, A. (2021). Recent Advances in Alkaline Exchange Membrane Water Electrolysis and Electrode Manufacturing. Molecules, 26(21), 6326.

Jang, D., Cho, H.-S., & Kang, S. (2021). Numerical modeling and analysis of the effect of pressure on the performance of an alkaline water electrolysis system. International Journal of Hydrogen Energy, 46(4), 3061-3074.

Shiva Kumar, S., & Himabindu, V. (2019). Hydrogen production by PEM water electrolysis – A review. Materials Science for Energy Technologies, 2(3), 442-454.

Carmo, M., Fritz, D. L., Mergel, J., & Stolten, D. (2013). A comprehensive review on PEM water electrolysis. International Journal of Hydrogen Energy, 38(12), 4901–4934.

Foit, S., Ziegler, N., & Friedrich, K. (2020). Recent advances in alkaline electrolysis: Performance improvement and cost reduction. International Journal of Hydrogen Energy, 45(8), 5093–5108.

Guerra, O. J., Batista, A. M., & Torres, M. G. (2020). Advances in solid oxide electrolysis technology: A review. International Journal of Hydrogen Energy, 45(35), 17645–17659.

Huang, Y., He, C., Zhang, X., & Zhang, D. (2021). Recent developments in catalyst materials for proton exchange membrane electrolysis. Energy Reports, 7, 2053–2063.

Vasquez, M. L., Callaway, D., & Soder, L. (2020). Energy storage systems and their integration with renewable energy sources. Renewable and Sustainable Energy Reviews, 120, 109632.

Zeng, K., & Zhang, D. (2022). Recent advances in water electrolysis for hydrogen production: An overview. International Journal of Hydrogen Energy, 47(26), 13528–13545.

Younas, M., Shafique, S., Hafeez, A., Javed, F., & Rehman, F. (2022). An overview of hydrogen production: Current status, potential, and challenges. Fuel, 316, 123317. https://doi.org/10.1016/j.fuel.2022.123317

Gençer, E. (2021, June 23). Hydrogen. MIT Climate Portal. https://climate.mit.edu/explainers/hydrogen access at 25/03/2025

Zhang, B., Zhang, S. X., Yao, R., Wu, Y. H., & Qiu, J. S. (2021). Progress and prospects of hydrogen production: Opportunities and challenges. Journal of Electronic Science and Technology, 19, 100080. https://doi.org/10.1016/j.jnlest.2021.100080

Ahn, S.-Y., Kim, K.-J., Kim, B.-J., Hong, G.-R., Jang, W.-J., Bae, J. W., Park, Y.-K., Jeon, B.-H., & Roh, H.-S. (2023). From gray to blue hydrogen: Trends and forecasts of catalysts and sorbents for unit process. Renewable and Sustainable Energy Reviews, 186, 113635. https://doi.org/10.1016/j.rser.2023.113635

AlHumaidan, F. S., Absi Halabi, M., Rana, M. S., & Vinoba, M. (2023). Blue hydrogen: Current status and future technologies. Energy Conversion and Management, 283, 116840. https://doi.org/10.1016/j.enconman.2023.116840

Amini Horri, B., & Ozcan, H. (2024). Green hydrogen production by water electrolysis: Current status and challenges. Current Opinion in Green and Sustainable Chemistry, 47, 100932. https://doi.org/10.1016/j.cogsc.2023.100932

Franco, A., & Giovannini, C. (2023). Recent and future advances in water electrolysis for green hydrogen generation: Critical analysis and perspectives. Sustainability, 15, 16917. https://doi.org/10.3390/su151816917

El-Shafie, M. (2023). Hydrogen production by water electrolysis technologies: A review. Results in Engineering, 20, 101426. https://doi.org/10.1016/j.rineng.2023.101426

Nasser, M., Megahed, T. F., Ookawara, S., & Hassan, H. (2022). A review of water electrolysis–based systems for hydrogen production using hybrid/solar/wind energy systems. Environmental Science and Pollution Research, 29, 86994–87018. https://doi.org/10.1007/s11356-022-21720-4

Brauns, J., & Turek, T. (2020). Alkaline water electrolysis powered by renewable energy: A review. Processes, 8, 248. https://doi.org/10.3390/pr8020248

Burton, N. A., Padilla, R. V., Rose, A., & Habibullah, H. (2021). Increasing the efficiency of hydrogen production from solar powered water electrolysis. Renewable and Sustainable Energy Reviews, 135, 110255. https://doi.org/10.1016/j.rser.2020.110255

Jaradat, M., Alsotary, O., Juaidi, A., Albatayneh, A., Alzoubi, A., & Gorjian, S. (2022). Potential of producing green hydrogen in Jordan. Energies, 15, 9039. https://doi.org/10.3390/en15239039

Budama, V. K., Rincon Duarte, J. P., Roeb, M., & Sattler, C. (2023). Potential of solar thermochemical water-splitting cycles: A review. Solar Energy, 249, 353–366. https://doi.org/10.1016/j.solener.2022.12.028

Warren, K. J., & Weimer, A. W. (2022). Solar thermochemical fuels: Present status and prospects. Solar Compass, 1, 100010. https://doi.org/10.1016/j.solcom.2022.100010

Das, A., & Peu, S. D. (2022). A comprehensive review on recent advancements in thermochemical processes for clean hydrogen production to decarbonize the energy sector. Sustainability, 14, 11206. https://doi.org/10.3390/su141811206

Boretti, A. (2022). Which thermochemical water-splitting cycle is more suitable for high-temperature concentrated solar energy? International Journal of Hydrogen Energy, 47, 20462–20474. https://doi.org/10.1016/j.ijhydene.2022.04.291

Rehman, H. (2023). Electronic and surface modifications of Ni–Co–Fe oxides: A catalyst with maximum exposure of Fe active sites for water electrolysis. ACS Applied Energy Materials. https://doi.org/10.1021/acsaenm.2c00257

Sugawara, Y., Miyanishi, S., Illathvalappil, R., Gangadharan, P. K., Kuroki, H., Anilkumar, G., et al. (2023). Anion exchange membrane water electrolyzers: An overview. Journal of Chemical Engineering of Japan, 56(1). https://doi.org/10.1080/00219592.2023.2210195

Liang, S.-H., Ma, Y., Luo, H., Wu, K., Chen, J., & Yang, J. (2023). A membrane-free decoupled water electrolyzer operating at simulated fluctuating renewables with tri-functional NiCo-P electrode. Chemistry – A European Journal. https://doi.org/10.1002/chem.202302160

Selvam, C., Devarajan, Y., Raja, T., & Vickram, S. (2025). Advancements in water electrolysis technologies and enhanced storage solutions for green hydrogen using renewable energy sources. Applied Energy, 390, 125849. https://doi.org/10.1016/j.apenergy.2025.125849

Genovese, M., Schlüter, A., Scionti, E., Piraino, F., Corigliano, O., & Fragiacomo, P. (2023). Power-to-hydrogen and hydrogen-to-X energy systems for the industry of the future in Europe. International Journal of Hydrogen Energy, 48(44), 16545–16568. https://doi.org/10.1016/j.ijhydene.2023.01.194

Alhadhrami, K., Albalawi, A., Hasan, S., & Elshurafa, A. M. (2024). Modeling green hydrogen production using power-to-x: Saudi and German contexts. International Journal of Hydrogen Energy, 64, 1040–1051. https://doi.org/10.1016/j.ijhydene.2024.03.161

Matheswaran, M. M. (2023). Effective integration and technical feasibility analysis of solar thermal networks for industrial process heating applications. In CRC Press eBooks (pp. 237–255). https://doi.org/10.1201/9781003263326-12

Boretti, A. (2020). Production of hydrogen for export from wind and solar energy, natural gas, and coal in Australia. International Journal of Hydrogen Energy, 45(7), 3899–3904.

Neofytidis, C., Ioannidou, E., Sygellou, L., Kollia, M., & Niakolas, D. K. (2023). Affecting the H_2O electrolysis process in SOECs through modification of NiO/GDC; experimental case of Au-Mo-Ni synergy. International Journal of Hydrogen Energy, 48(46), 17711–17728.

Vilbergsson, K. V., Dillman, K., Emami, N., Ásbjörnsson, E. J., Heinonen, J., & Finger, D. C. (2023). Can remote green H_2 production play a key role in decarbonizing Europe in the future? A cradle-to-gate LCA of H_2 production in Austria, Belgium, and Iceland. International Journal of Hydrogen Energy, 48(46), 17711–17728.

Ahanem, M., Mellit, A., Almohamadi, H., Haddad, S., Chettibi, N., Alanazi, A. M., … Alzahrani, A. (2023). H_2 production methods based on solar and wind energy: A review. Energies, 16(2), 757.

Ioannidou, E., Neofytidis, C., Sygellou, L., & Niakolas, D. K. (2018). Au-doped Ni/GDC as an improved cathode electrocatalyst for H_2O electrolysis in SOECs. Applied Catalysis B: Environmental, 236, 253–264.

Bhattacharyya, R., Misra, A., & Sandeep, K. C. (2017). Photovoltaic solar energy conversion for H_2 production by alkaline water electrolysis: Conceptual design and analysis. Energy Conversion and Management, 133, 1–13.

Carlson, E. L., Pickford, K., & Nyga-Łukaszewska, H. (2023). Green H_2 and an evolving concept of energy security: Challenges and comparisons. Renewable Energy, 219, 119410.

Gholami, T., & Pirsaheb, M. (2021). Review of effective parameters in electrochemical H_2 storage. International Journal of Hydrogen Energy, 46(1), 783–795.

Kiessling, A., Fornaciari, J. C., Anderson, G. A., Peng, X., Gerstmayr, A., Gerhardt, M. R., McKinney, S., Serov, A., Kim, Y. S., Zulevi, B., Weber, A. Z., & Danilovic, N. (2021). Influence of supporting electrolyte on hydroxide exchange membrane water electrolysis performance: Anolyte. Journal of The Electrochemical Society, 168(8), 084512.

Arat, H. T., Baltacioglu, M. K., Tanç, B., Sürer, M. G., & Dincer, I. (2020). A perspective on hydrogen energy research, development and innovation activities in Turkey. International Journal of Energy Research, 44(2), 588–593.

Ding, H., Wu, W., Jiang, C., Ding, Y., Bian, W., Hu, B., Singh, P., Orme, C. J., Wang, L., Zhang, Y., & Ding, D. (2020). Self-sustainable protonic ceramic electrochemical cells

using a triple conducting electrode for H_2 and power production. Nature Communications, 11(1), 1–8.

Habour, R. M., Benyounis, K. Y., & Carton, J. G. (2025). Green hydrogen production from renewable sources for export. International Journal of Hydrogen Energy, 128, 760–770. https://doi.org/10.1016/j.ijhydene.2025.04.291

Camargo, J., White, J., & Hamon, F. (2024). Managing reservoir dynamics when converting natural gas fields to underground hydrogen storage. International Journal of Hydrogen Energy. [Online] Elsevier. https://www.sciencedirect.com/science/article/pii/S0360319923047808 access at 02/04/2025

Dufo-López, R., Lujano-Rojas, J. M., Bernal-Agustín, J. L., Artal-Sevil, J. S., & Bayod-Rújula, Á. A. (2024). Stable hydrogen generation by wind power, grid, and battery. Renewable Energy and Power Quality Journal. https://doi.org/10.24084/reepqj24.394

Mishra, A., Park, H., El-Mellouhi, F., & Han, D. S. (2024). Seawater electrolysis for hydrogen production: Technological advancements and future perspectives. Fuel, 361, 130636. https://doi.org/10.1016/j.fuel.2023.130636

Haq, T. U., & Haik, Y. (2022). Strategies of anode design for seawater electrolysis: Recent development and future perspective. Small Science, 2(9), 2200030. https://doi.org/10.1002/smsc.202200030

Gao, F.-Y., Yu, P.-C., & Gao, M.-R. (2022). Seawater electrolysis technologies for green hydrogen production: Challenges and opportunities. Current Opinion in Chemical Engineering, 36, 100827. https://doi.org/10.1016/j.coche.2022.100827

Rahmouni, S., Settou, N., Chennouf, N., Negrou, B., & Houari, M. (2014). A technical, economic and environmental analysis of combining geothermal energy with carbon sequestration for H_2 production. Energy Procedia, 50, 263–269.

Hindson, W. A., & James, S. (2024). Effects of surface modification on a proton exchange membrane for improvements in green H_2 production. International Journal of Hydrogen Energy, 49, 1040–1047.

Rahmouni, S., Settou, N., Chennouf, N., Negrou, B., & Houari, M. (2014). A technical, economic and environmental analysis of combining geothermal energy with carbon sequestration for H_2 production. Energy Procedia, 50, 263.

Mitzel, J., & Friedrich, K. A. (2021). Hydrogen fuel cell applications. In Utilization of Hydrogen for Sustainable Energy and Fuels (Vol. 367).

Al-Gamal, A. G., Yehia, F., Elmasry, M. R., Abo El-Khair, M. A., Kandeel, H. S., Elseman, A. M., Kim, D.-H., & Kabel, K. I. (2024). Perovskite materials for hydrogen evolution: Processes, challenges and future perspectives. International Journal of Hydrogen Energy, 79, 1113–1138. https://doi.org/10.1016/j.ijhydene.2024.07.039

Shang, Q., Piercy, B. D., Losego, M. D., & Lian, T. (2019). Effect of surface ligand on charge separation and recombination at $CsPbI_3$ perovskite quantum dot/TiO_2 interfaces. Journal of Physical Chemistry C, 123, 21415–21421.

European Commission. (2024). Hydrogen. Energy - European Commission. https://energy.ec.europa.eu/topics/eus-energy-system/hydrogen_en access at 06/03/2025

Iberdrola. (n.d.). Puertollano green hydrogen plant. https://www.iberdrola.com/about-us/what-we-do/green-hydrogen/puertollano-green-hydrogen-plant access at 10/04/2025

European Commission. (2020). A hydrogen strategy for a climate-neutral Europe (COM/2020/301 final). EUR-Lex. https://eur-lex.europa.eu/legal-content/EN/TXT/?uri=CELEX:52020DC0301

Bhuiyan, M. M. H., & Siddique, Z. (2025). Hydrogen as an alternative fuel: A comprehensive review of challenges and opportunities in production, storage, and transportation. International Journal of Hydrogen Energy, 102, 1026–1044. https://doi.org/10.1016/j.ijhydene.2025.01.033

Ren, S., Jia, X., Wang, S., He, P., Zhang, S., & Peng, X. (2024). Creation and validation of a dynamic simulation method for the whole process of a hydrogen refueling station. Journal of Energy Storage, 82, 110508. https://doi.org/10.1016/j.est.2024.110508

Sánchez, M., Amores, E., Abad, D., Rodríguez, L., & Clemente-Jul, C. (2020). Aspen Plus model of an alkaline electrolysis system for hydrogen production. International Journal of Hydrogen Energy, 45(7), 4141–4154. https://doi.org/10.1016/j.ijhydene.2019.12.123

AspenTech. (2025). Aspen Plus® V15 Help Documentation. Aspen Technology, Inc.

Li, X. (2007). Thermodynamic performance of fuel cells and comparison with heat engines. In T. S. Zhao, K.-D. Kreuer, & T. V. Nguyen (Eds.), Advances in fuel cells (Vol. 1, pp. 1–46). Elsevier Science. https://doi.org/10.1016/S1752-301X(07)80006-8

Barbir, F. (2013). Main cell components, material properties, and processes (Chapter 4). In F. Barbir (Ed.), PEM fuel cells (2nd ed., pp. 73–117). Academic Press. https://doi.org/10.1016/B978-0-12-387710-9.00004-7

Bi, X., Wang, G., Cui, D., Qu, X., Shi, S., Yu, D., Cheng, M., & Ji, Y. (2025). Simulation study on the effect of temperature on hydrogen production performance of alkaline electrolytic water. International Journal of Hydrogen Energy. https://doi.org/10.1016/j.ijhydene.2023.12.242